ERDC/CRREL TR-22-23

Cold Regions Research and Engineering Laboratory

US Army Corps of Engineers®
Engineer Research and Development Center

ERDC
ENGINEER RESEARCH & DEVELOPMENT CENTER

Cold Regions Vehicle Start

Next-Generation Lithium-Ion Battery Technologies for Stryker Vehicles

Kathryn P. Trubac, Randall W. Reynolds, Timothy J. Cooke, Caylin A. Hartshorn, Douglas A. Punt, Christopher J. Donnelly, and Caitlin A. Callaghan

November 2022

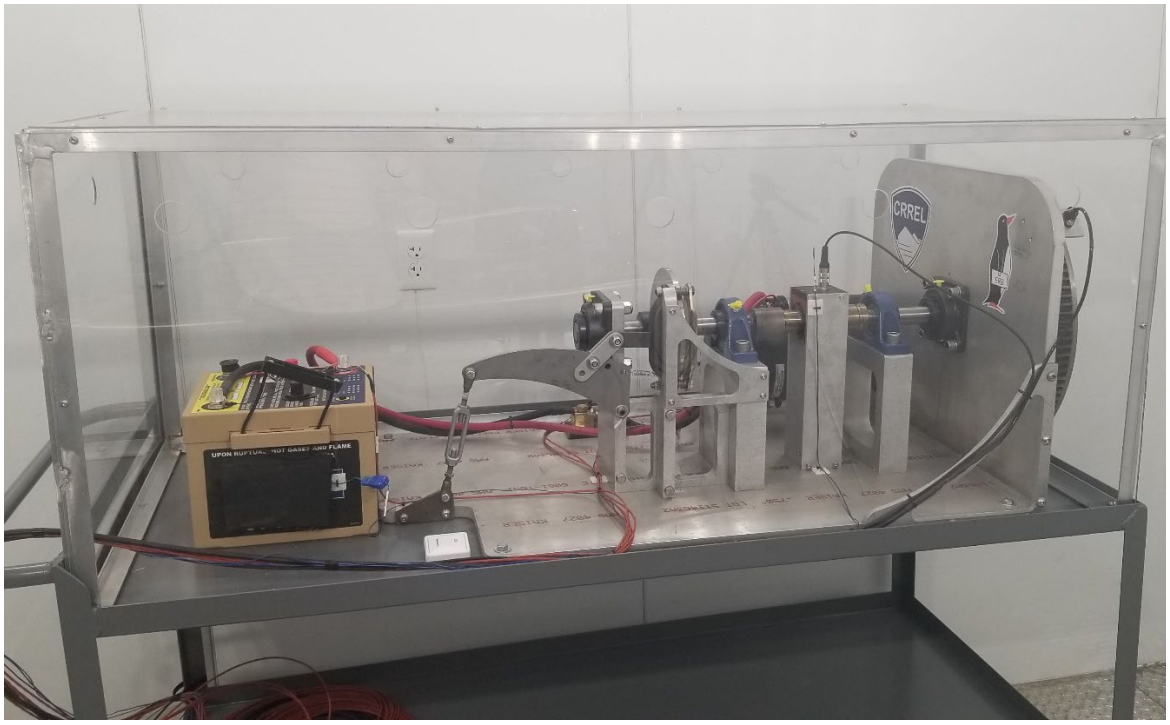

The US Army Engineer Research and Development Center (ERDC) solves the nation's toughest engineering and environmental challenges. ERDC develops innovative solutions in civil and military engineering, geospatial sciences, water resources, and environmental sciences for the Army, the Department of Defense, civilian agencies, and our nation's public good. Find out more at www.erdc.usace.army.mil.

To search for other technical reports published by ERDC, visit the ERDC online library at https://erdclibrary.on.worldcat.org/discovery.

ERDC/CRREL TR-22-23
November 2022

Cold Regions Vehicle Start

Next-Generation Lithium-Ion Battery Technologies for Stryker Vehicles

Kathryn P. Trubac, Randall W. Reynolds, Timothy J. Cooke, Caylin A. Hartshorn, Douglas A. Punt, Christopher J. Donnelly, and Caitlin A. Callaghan

US Army Engineer Research and Development Center (ERDC)
Cold Regions Research and Engineering Laboratory (CRREL)
72 Lyme Road
Hanover, NH 03755-1290

Final Technical Report (TR)

Prepared for Headquarters, US Army Corps of Engineers
Washington, DC 20314-1000

Under PE 0603119A, "Ground Advanced Technology," Project B03, "Military Engineering Technology Demonstration," Tasks SB0307 and SB0348, "Energy Technology Research in Cold and Arctic Regions"

Abstract

Operating vehicles in extremely cold environments is a significant problem for not only the public but also the military. The Department of Defense has encountered issues when trying to reliably cold start large, heavy-duty military vehicles, specifically the M1126 Stryker Combat Vehicle, in cold regions. As noted in previous work, the issue stems from the current battery technology's limited temperature range. This current project utilized the protocol established in the previous phase to evaluate next-generation lithium-ion battery technologies for use in cold regions. Selected battery technologies met necessary military specifications for use in large military combat vehicles and were evaluated using a mechanical load system developed in previous work to simulate the starting of a Stryker engine. This work also evaluated the performance of the existing battery technology of a Stryker under Alaskan winter temperatures, which will verify the accuracy of the simulated cold room testing on the mechanical load system. The results of the tests showed that while the system was able to reliably operate down to –20°C, the battery management system encountered challenges at the lower end of the temperature range. This technology has a potential to reliably support cold regions operations but needs further evaluation.

Contents

Figures and Tables

Figures

Tables

Preface

This study was conducted for the US Army Corps of Engineers under PE 0603119A, "Ground Advanced Technology," Project B03, "Military Engineering Technology Demonstration," Tasks SBO307 and SBO348, "Energy Technology Research in Cold and Arctic Regions." The technical monitors were Ms. Danielle Kennedy and Dr. Thomas Douglas, US Army Engineer Research and Development Center, Cold Regions Research and Engineering Laboratory (ERDC-CRREL).

The work was performed by the Engineering Resources Branch of the Research and Engineering Division, ERDC-CRREL. At the time of publication, Dr. Melisa Nallar was acting branch chief; Dr. Caitlin A. Callaghan was division chief; and Mr. David Ringelberg was the technical director for Cold Regions Science and Engineering. The acting deputy director of ERDC-CRREL was Mr. Bryan E. Baker, and the director was Dr. Joseph L. Corriveau.

COL Christian Patterson was commander of ERDC, and Dr. David W. Pittman was the director.

1 Introduction

1.1 Background

Operating vehicles and machinery in extremely cold environments is a significant problem for not only the public but also the military. The DoD has encountered many issues when trying to reliably cold start large, heavy-duty military vehicles in cold regions. One system specifically challenged by low temperatures is the M1126 Stryker Combat Vehicle. The US Army Alaska 1-25th Stryker Brigade Combat Team (SBCT; Figure 1) stationed at Fort Wainwright, Alaska, has concerns regarding their current battery and starter system and its ability to operate when exposed to the low temperatures experienced in this location.

Figure 1. The 1-25th Stryker Brigade Combat Team in Fort Wainwright, Alaska. (Image reproduced from US Army Alaska 2020. Public domain.).

As noted in previous work (Trubac et al. 2022), the issue stems from the current battery technology's limited temperature range. Lead-acid batteries are the most common chemistry used in vehicles; however, they are severely impacted by decreasing temperatures. To mitigate this issue and improve the reliability of cold starting Strykers, a team at the US Army Engineer Research and Development Center's Cold Regions Research and Engineering

Laboratory (ERDC-CRREL) investigated next-generation lithium-ion battery technologies and temperature's effect on their performance.

1.2 Objective

The objective for this project was to evaluate next-generation lithium-ion vehicle-battery technologies under extreme cold conditions to gain an understanding of the batteries' performances with respect to temperature. The goal was to compare performance of these battery technologies to the currently used ultracapacitor engine start module (evaluated in a previous project) and to identify any improvements made by certain technologies. In addition, this work evaluated the performance of the existing lead-acid battery system of the Stryker for comparison. This was to verify the accuracy of the CREEL battery test equipment and to identify whether the next-generation lithium-ion batteries showed any improvements over the lead-acid batteries.

1.3 Approach

This work was accomplished by a team at CRREL due to the member's experience and prior research efforts related to this work. Leveraging existing cold facilities and battery-evaluation equipment, the team set up the necessary instrumentation and collected data on battery performance throughout the project. In addition to analyzing the results and documenting the findings, team members traveled to Fort Wainwright to communicate with the 1-25th SBCT and to gain information on the operation of the existing Stryker battery system in real-world cold conditions.

1.4 Impact to the Army

The US military has a large investment in the cold regions of the US, with 21,407 active-duty military personnel stationed in Alaska, of which the Army makes up 51% (Alaska Department of Labor and Workforce Development 2020). Figure 2 shows the distribution of military personnel by branch. The unique conditions experienced in the nation's cold regions lead to many operational and technical challenges.

Figure 2. Active-duty military population in Alaska by branch in 2019. (Image reproduced with permission from Alaska Department of Labor and Workforce Development 2020).

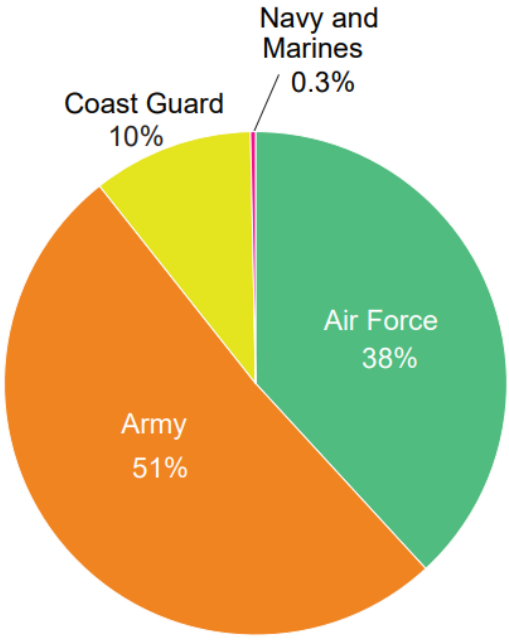

An installation's ability to reliably start its vehicles is imperative to emergency response and mission success. Investigating and identifying improvements to Army vehicle cold-start capabilities ensure that personnel will be prepared no matter the conditions. As stated in Trubac et al. (2022), improving cold-start capabilities will eliminate the need to remove batteries from the vehicle to warm and the need to leave the vehicle running, saving both time and effort. This also prevents the risk of prolonged exposure of personnel to extreme temperatures and limits the fuel needed and the exhaust produced while the vehicle is idling.

This work is intended to provide guidance on the optimal battery technology for use in military vehicles in cold regions; however, the results obtained from this study have the potential to also inform nonmilitary efforts related to battery and vehicle use in cold environments.

2 Technology Review

2.1 Current technology

There are many varieties of batteries, and the differences come down to the materials used in production and how the battery was constructed. Batteries are usually grouped together according to the main constituents, such as lead-acid or lithium-ion, but there are many varieties within those groups. In addition to that, there are other energy storage technologies that have potential for use in vehicles, such as ultracapacitors. The following sections discuss some of the different available technologies.

2.1.1 Lead-acid batteries

Lead-acid batteries, like all batteries, rely on a chemical process. They are made of lead-based electrodes that are separated by a liquid electrolyte. The electrolyte is a blended solution of sulfuric acid (Bukhari 2015). In general, lead-acid batteries are outperformed in most categories by lithium-ion batteries, which have a higher power density, energy density, and lifespan (Bukhari 2015). Still, manufacturing costs are significantly lower than for other chemistries, ranging from several hundred to several thousand dollars cheaper than lithium-ion batteries. This has allowed lead-acid batteries to keep a share of the market (Hutchinson 2004).

2.1.2 Ultracapacitors

Ultracapacitors are like batteries in the sense that they are composed of a positive and a negative electrode and store energy by placing a positive charge on one electrode and a negative charge on the other. However, the two electrodes of an ultracapacitor are separated by a porous separator, usually made of carbon or graphite (shown in Figure 3), as opposed to being immersed in an electrolyte (Berrueta et al. 2019).

Figure 3 . Schematic of an ultracapacitor.

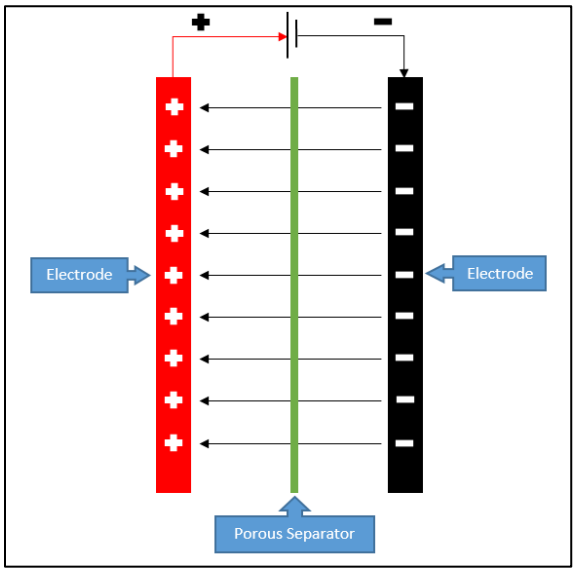

Trubac et al. (2022) investigated ultracapacitors to assist starting military vehicles. The Maxwell 24 V* heavy-duty engine start module (ESM) is a technology composed of several cells of ultracapacitors that could be installed in the starter system of a large, heavy-duty vehicle to improve the vehicle's ability to start at extreme low temperatures (Figure 4).

Figure 4. Maxwell Technology's 24 V heavy-duty ultracapacitor engine start module.

During testing, Trubac et al. (2022) determined that, while this technology was able to start a simulated Stryker engine at temperatures down to

* For a full list of the spelled-out forms of the units of measure used in this document and their conversions, please refer to US Government Publishing Office Style Manual, 31st ed. (Washington, DC: US Government Publishing Office, 2016), 248–252 and 345–347, https://www.govinfo.gov/content/pkg/GPO-STYLEMANUAL-2016/pdf/GPO-STYLEMANUAL-2016.pdf.

−40°C, the ultracapacitor ESM was suited only for starting the engine. Because of the technology's low energy density, the ultracapacitor ESM is not designed to support any sustained auxiliary load, such as additional sensors or equipment.

2.2 Lithium-ion batteries

Lithium-ion is a classification of batteries that are made with metal lithium. This material classification is used to distinguish them from lead-acid batteries. There are many different active materials used to create different lithium-ion chemistries. The term *lithium-ion* actually encompasses several different individual battery chemistries. While they all share similar characteristics, each chemistry has different applications and limitations. For example, some chemistries are better suited for operation in cold conditions, and some are less expensive.

2.2.1 Lithium-ion battery chemistries

2.2.1.1 Lithium cobalt oxide ($LiCoO_2$)

One of the most common lithium-ions is lithium cobalt oxide ($LiCoO_2$), LCO. As the name suggests, cobalt is the active material, where lithium ions are sandwiched between anionic sheets of cobalt and oxygen (Shao-Horn 2003). This type of chemistry, or blended variations of it, has been at the top of the market for years due to high energy density, ease of manufacturing, and low maintenance required. However, it comes with some significant disadvantages. Cobalt has a high financial cost and also comes with certain human rights costs associated with the mining. Although LCO has a very high energy density, it is fairly limited in power density (University of Texas at Austin 2020). It is great for lower-current applications, such as cell phones, computers, and cameras; but it is not ideal for high-current applications, such as starter batteries, portable power tools, and unmanned aerial vehicles.

2.2.1.2 Lithium titanate (Li_2TiO_3)

Lithium titanate (Li_2TiO_3) batteries differ from other lithium-ion batteries by replacing a carbon anode with lithium titanate (Wang et al. 2017). The cathode can be made of lithium manganese oxide or lithium manganese cobalt. These batteries are known for high thermal stability, high charge and discharge rates, safety, and endurance. However, lithium titanate batteries have a low nominal voltage (2.4 V) and low specific energy (30–

100 Wh/kg) with respect to other batteries (Cowie 2015). Typically, these batteries can be found in uninterruptable power supplies; electric power trains; solar streetlights; and, recently, mobile medical devices (Battery University 2021; Cowie 2015). With the high cost of the materials needed for construction (titanium and cobalt), lithium titanate batteries are at another disadvantage compared to other chemistries.

2.2.1.3 Lithium iron phosphate ($LiFePO_4$)

Lithium iron phosphate ($LiFePO_4$) batteries consist of an electrolyte medium, a carbon anode, and a lithium iron phosphate cathode. A single battery cell nominal voltage measures 3.2 V. This specific cathode material provides energy densities greater than 175 Wh/kg in addition to safety and durability (Li and Ma 2019). Furthermore, $LiFePO_4$ stays stable over large ranges of temperatures and cycles, increasing its popularity for electric vehicles and electric grid storage (Satyavani et al. 2016). Additionally, the four-cell lithium iron phosphate battery provides a convenient replacement for the lead-acid battery since the lithium iron phosphate battery has a nominal voltage of 12.4 V (Lam 2020). Since the battery does not use expensive materials like nickel or cobalt, the battery prices are lower than other lithium-ion batteries (Li and Ma 2019). One disadvantage of lithium iron phosphate is low electrical conductivity (~10^{-9} to 10^{-10} S cm^{-1}) compared to LCO (~10^{-3} to 10^{-4} S cm^{-1}). This battery property decreases the charge and discharge rate capacity, but several advances have been made to electrical conductivity in recent years (Satyavani et al. 2016).

2.2.1.4 Lithium mixed metal oxides

Other less prominent lithium-ion battery chemistries include lithium mixed metal oxide batteries. Mixed metal oxide batteries encompass several chemistries that vary depending on the composition of the metals used in the battery. For example, two slight variations of LCO have recently gained popularity—lithium nickel manganese cobalt oxide and lithium nickel cobalt aluminum oxide. They retain many of the benefits of LCO while reducing the amount of cobalt used and improving battery performance (University of Texas at Austin 2020). The specific application of each chemistry varies as each technology is at a different stage of development, but many of these mixed metal batteries have the potential to be utilized in vehicles in the future.

2.3 Battery cold performance challenges

Temperature extremes pose many challenges for batteries. The optimum operating temperature for lead-acid batteries is 25°C (Hutchinson 2004). All batteries store energy by taking advantage of an electrochemical reaction to produce the electric potential. This is different from an ultracapacitor, which stores energy physically as a surface charge, electrostatically (Liu et al. 2009). Temperature greatly affects these chemical reactions. Higher temperature extremes will excite the electrons, increasing the conductivity. This increases the capacity of the battery, which in turn significantly decreases the overall life. Low-temperature extremes have the opposite effect, where electrons are excited less than expected. This decrease in conductivity increases the internal resistance of the battery. The increase in resistance limits the amount of energy that can be extracted, thus decreasing the overall capacity of the battery (Jaguemont et al. 2015). This decreased capacity as a function of temperature is not linear. For lead-acid batteries, using a common discharge rate of 0.10°C, battery capacity drops to approximately 80% at 0°C, 60% at –20°C, and 30% at –40°C (Hutchinsion 2004). Because all batteries rely on chemical reactions, they all suffer degradation when operating in a cold environment. However, cold does not affect all chemistries to the same degree. Low-temperature extremes do affect the performance of lithium-ion batteries but at a significantly lower rate than for lead-acid batteries. At a temperature of –10°C, lithium-ion batteries provided 5.2 and 8.5 times the capacity of lead-acid batteries at a discharge rate of 30 A and 50 A respectively (Battle Born Batteries 2020).

2.4 MIL-PRF-32565B performance specification

The military creates standardization for nearly every item it uses. This is to ensure all similar parts are built with interchangeable tolerances and can be safely used for many different military applications. This is especially useful for emergency field repairs at forward operating bases.

For this particular research, the CRREL team used a Stryker vehicle as a base. These vehicles require the physical size of the battery to be a 6T standard as specified in STANAG 2601 (NATO 2017).

For the military to use a 6T-sized, rechargeable, lithium battery in a vehicle power system, they ensure the battery is built in such a way to achieve the characteristics described in the MIL-PRF-32565B performance document

(TARDEC 2019). MIL-PRF-32565B includes environmental, electrical, and mechanical attributes and references other documentation for any specific callouts required during fabrication, such as types of plastics, metals, and any special compatibility issues to nearby devices installed in the vehicle.

3 Methodology

The purpose of this work was to collect data on the performance of next-generation lithium-ion battery technologies for military vehicles, specifically the Stryker Combat Vehicle. The Stryker is the test case used in this work; however, platforms with similar requirements could use the technologies evaluated by these tests. The tests intended to replicate realistic cold-crank starting conditions of a large heavy-duty vehicle, based on MIL-PRF-32565B for 6T military lithium-ion batteries, outlined in Section 2.4 (TARDEC 2019). The batteries selected for testing were evaluated across the specified temperature range (Table 1) determined in Trubac et al. (2022).

Table 1. Selected temperatures for testing.

Temperature Range
28°C
18°C
0°C
−10°C
−20°C
−30°C
−40°C

This work aimed to identify changes in the batteries' performance according to temperature. By monitoring the variations in the voltage of the batteries as they were tested on the simulated load, the goal was to investigate if the cold negatively affects the ability of each battery to successfully start a Stryker engine.

3.1 Test battery selection

Before performing the tests, the team had to select the batteries to use. The batteries chosen for testing had to fulfill several requirements for the conditions the tests were emulating. Because the testing was to simulate cold starting a Stryker, the batteries had to meet the vehicle requirements for use in a Stryker, which the following sections outline.

3.1.1 Battery requirements

3.1.1.1 6T batteries

Batteries used in military vehicles have specific requirements. These vehicles require the physical size of the battery to be a 6T standard as specified in STANAG 2601 (NATO 2017). A 6T battery can be a lead-acid chemistry or a lithium-ion chemistry if it meets the NATO specifications. This was the minimum requirement for the batteries used in this work—they must fall within the 6T category for batteries.

3.1.1.2 MIL-PRF-32565B Batteries

As stated in Section 2.4, MIL-PRF-32565B contains "general requirements for secondary (rechargeable) nominal 24 volt lithium-ion (Li-ion) batteries having the 6T form factor in accordance with STANAG 4015" (STANAG 2601 [NATO 2017] replaced STANAG 4015; TARDEC 2019, 1). Batteries that meet these requirements are intended to be used as power sources for automotive starting, lighting, ignition, and auxiliary electronics. For the purposes of this work, this specification acted as a stricter set of characteristics that the lithium-ion batteries used for testing had to meet. While the batteries used in this work were required to meet all MIL-PRF-32565B specifications, there were several key characteristics that were critical for these tests. Table 2 shows the specific size and weight requirements for the batteries used. Figure 5 and Figure 6 give more details on the required dimensions of the batteries.

In addition to the size requirements, the operating temperature range was important for these particular tests. Because the purpose of this work was to characterize the battery's performance when exposed to low temperatures, it was critical that the batteries used for testing met the MIL-PRF-32565B requirement for operating temperatures of –46°C to 71°C.

Table 2. The 6T battery weight and size requirements (TARDEC 2019).

Characteristic	Values
Maximum Weight	30 kg
Maximum Width	266 ± 3 mm
Maximum Length	283 ± 3 mm
Maximum Height	230 mm

Figure 5. Top-view battery dimensions. (Image reproduced from TARDEC 2019. Public domain.)

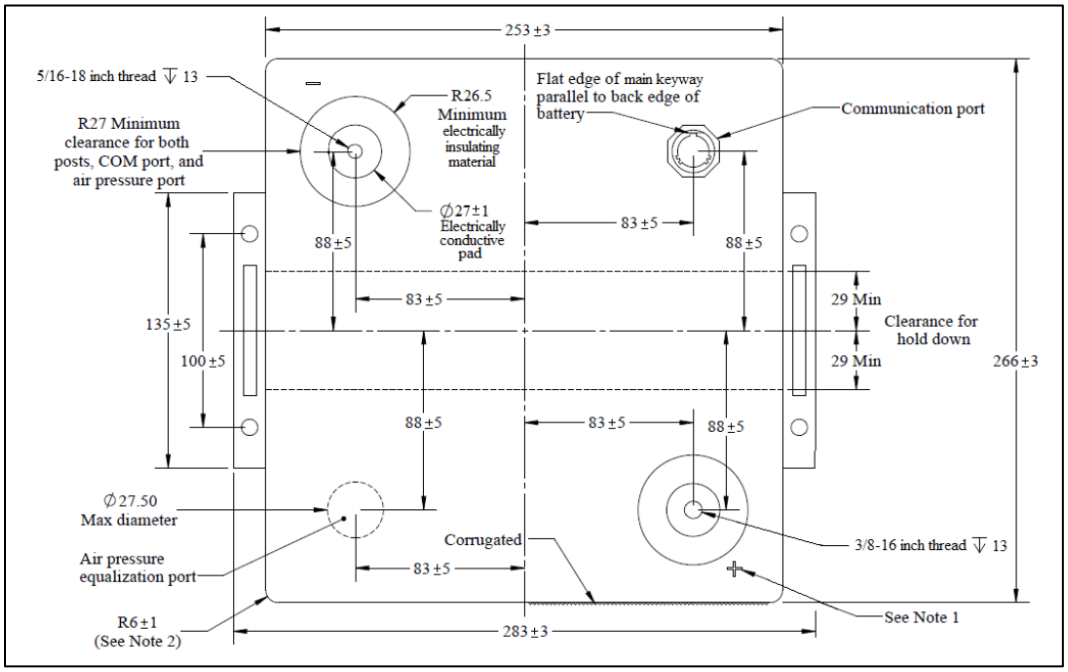

Figure 6. Side-view battery dimensions. (Image reproduced from TARDEC 2019. Public domain.)

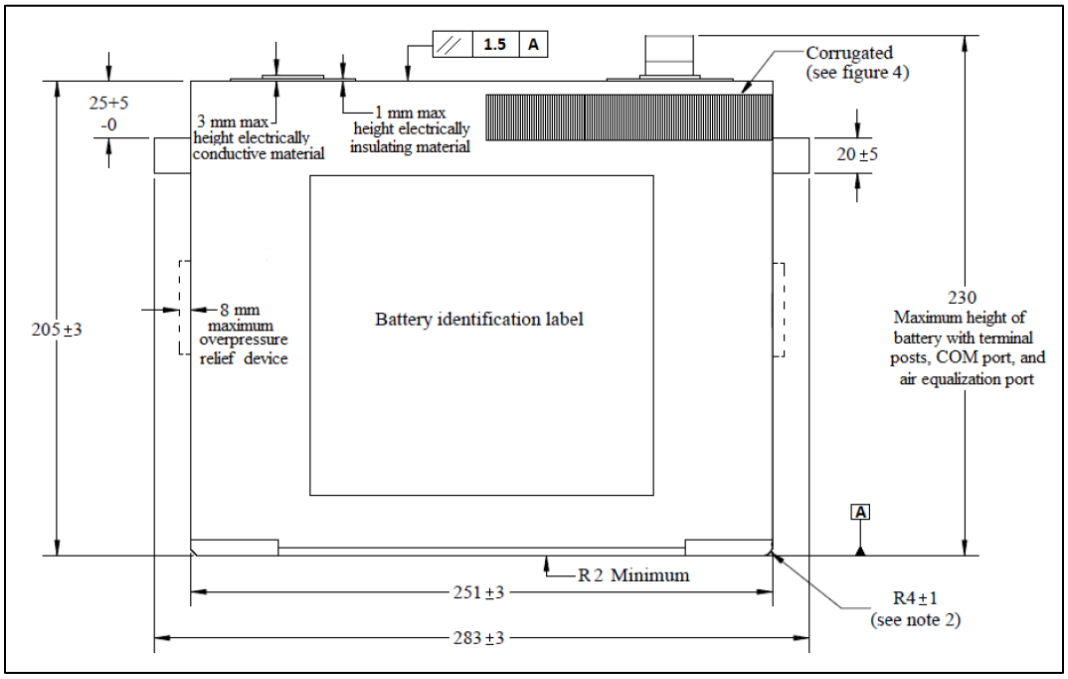

Because the testing investigated the battery's ability to cold start a Stryker, the requirements for cold-cranking amps (CCA) is also an important parameter to note (Table 3).

Table 3. Cold-cranking amp (CCA) requirements for Type 1-A 6T lithium-ion batteries (TARDEC 2019).

Temperature	CCA (No Preheating)
55°C	1100 A for 30 sec
−18°C	600 A for 30 sec
−32°C	300 A for 30 sec
−40°C	200 A for 30 sec

The battery selected for testing met all these requirements and was obtained from the manufacturer via a solicitation based on its compliance with MIL-PRF-32565B.

3.1.2 Bren-Tronics Inc. battery

The battery selected for testing was acquired through an open-source government solicitation for technologies that met the requirements of MIL-PRF-32565B. The battery technology evaluated in this work was the Brenergy BT-70939M-TPA/-TPB: 6T 24 V High-Power Li-Ion Battery manufactured by Bren-Tronics Inc. (Figure 7).

Figure 7. Bren-Tronics 24 V Brenergy lithium-ion battery.

3.2 Test Setup

3.2.1 CRREL cold room testing

Tests used a preestablished mechanical and electrical circuit configuration that contained a simulated load equivalent to a Stryker crank (Trubac et al. 2022), shown in Figure 8. The simulated load system was also instrumented with several sensors to monitor voltage, current, temperature, torque applied to the system, and rotational speed of components.

Figure 8. Mechanical load system in a CRREL cold room with the test battery connected.

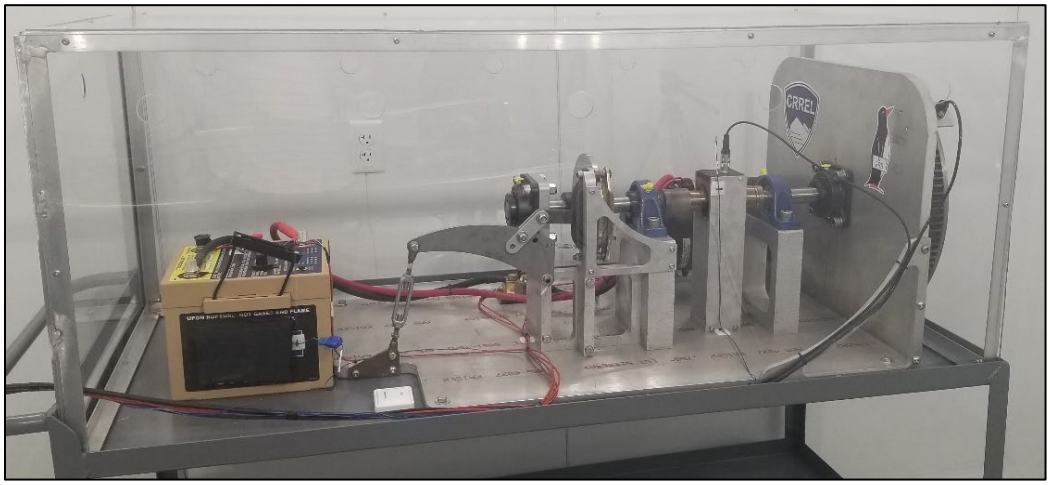

The entire test setup was installed in cold room CBx-21 to simulate the continuous cold soak conditions that the Stryker will experience in cold regions operations. All additional data collection equipment was set up outside the cold room. The same equipment and data collection devices from the previous work were used during these tests, only the lithium-ion batteries replaced the ultracapacitor ESM. Appropriate battery chargers were also used to recharge the batteries at ambient room temperature after completion of each temperature test.

With the lessons learned from the previous work with the ultracapacitor ESM, the team more closely monitored the mechanical brake system used to apply the appropriate torque to the load system and adjusted it prior to the second round of testing. This verified that the load system was consistently set to the correct torque value for each test, ensuring that the load simulation was an accurate representation of a Stryker engine.

3.2.2 Alaska field testing

For the field-testing component of this work, the CRREL team developed a portable data acquisition (DAQ) system for monitoring vehicle battery performance. This DAQ system was designed to collect data on various battery systems for many different purposes.

The DAQ was used in this work to evaluate the 12 V lead-acid Hawker batteries that were installed in the Stryker during the experiment.

3.2.2.1 Data acquisition

The DAQ system needed to synchronously record battery temperature, ambient temperature, battery voltage and battery current for two 24 V batteries at low temperatures. The minimum requirements were three thermocouple temperature measurements and four analog voltage measurements: two measurements for voltage and two measurements for current. As the scope of the testing covered both low-current constant draw and high-current CCA, two additional voltage measurements were needed for low-current measurements. This yielded six analog voltage measurements.

For the above-listed requirements, the National Instruments (NI) cDAQ-9178 was the best option. The NI cDAQ-9178 can hold eight NI C Series modules; these modules are capable to collecting analog voltage data, digital signal data, temperature data, controller area network bus data, and many more. All the data can be collected with two modules: the NI 9212 temperature module and the NI 9220 voltage module. These modules can record data from 8 thermocouples and 16 differential analog voltage channels, respectively. Additionally, the data acquisition system is rated to −20°C (NI 2016).

3.2.2.2 Voltage measurements

The Stryker vehicle uses two 24 V 6T batteries in parallel. The NI 9220 voltage module can directly measure ±10 V direct current (DC) with 16-bit resolution (1526 mV/bit) at 100 kHz; therefore, the voltage measurement needed to attenuate to the above-listed range for an accurate reading (NI 2022). A simple DC voltage reduction with minimal signal alteration is a voltage divider. This circuit reduced the input voltage following the equation below.

$$\frac{V_{\text{Out}}}{V_{\text{In}}} = \frac{R_k}{\sum_i^n R_i} = \frac{R_2}{R_2 + 2R_1}, \quad (1)$$

where

V_{Out} = the sensing voltage proportional to the battery voltage,
V_{In} = the battery voltage,
n = the number of resistors,
k = a number in the range 1 to n,
R_k = the resistor corresponding to sensing voltage,
R_i = any resistor in the voltage divider,
R_1 = the two resistors with a 15 kΩ value used to reduce voltage, and
R_2 = the sensing resistor with a 10 kΩ value.

The voltage divider in Figure 9 performed this voltage reduction with three resistors in series. The specific resistor used to quantify the battery voltage, R_2, was 10 kΩ and two other resistors reducing the voltage, R_1, were 15 kΩ. Because the other two resistors shared the same value, they were referenced as R_1. The three resistors produced a voltage and a voltage reduction, $V_{\text{Out}}/V_{\text{In}}$, across R_2 of 75%; a fully charged battery with a nominal voltage of 30 V DC would measure 7.5 V DC for the analog voltage module, which is well within the ±10 V DC range of the voltage module (Trubac et al. 2022). Also, the schematic in Figure 9 shows two voltage dividers as there were two batteries.

Figure 9. Data acquisition (DAQ) voltage-divider schematic.

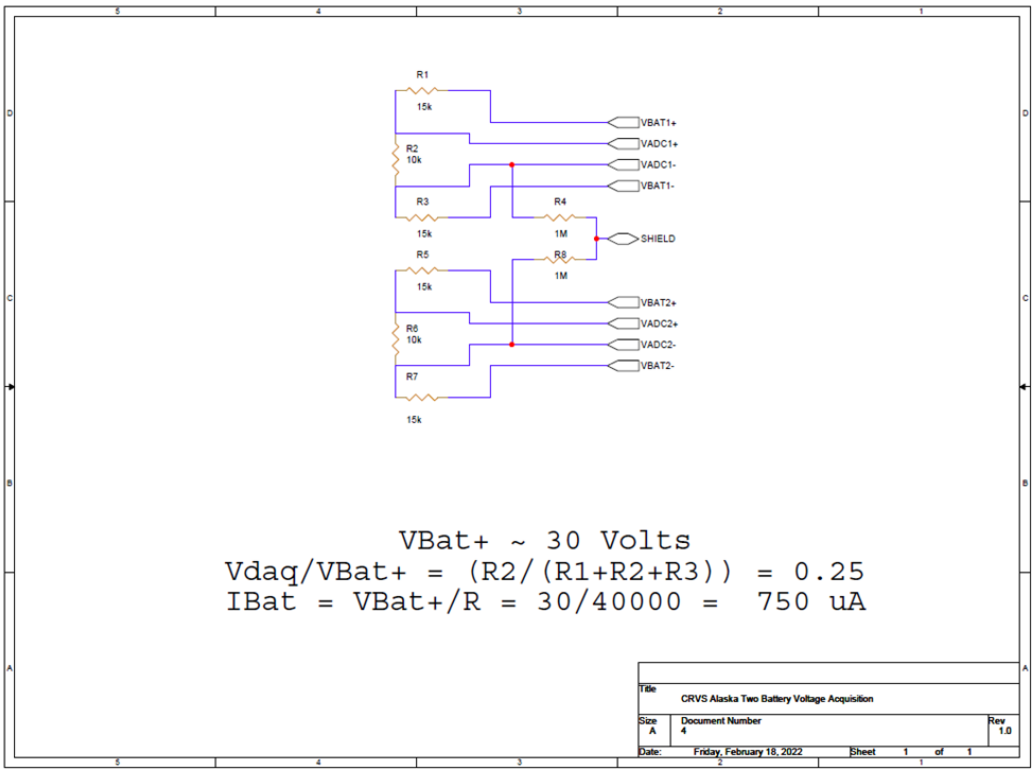

3.2.2.3 Current measurements

As mentioned above, there are two types of current measurements: low-current constant draw and high-current CCA. Therefore, two different circuits, designed for two different current ranges, transduced the current to an analog voltage. Both current transducers selected use a closed-loop Hall effect to measure current.

A closed-loop Hall effect sensor can measure AC (alternating current) or DC currents using a perpendicular current when in the presence of an applied magnetic field. In both cases, the wire provides an external magnetic field proportional to the wire current as given by the Biot-Savart law. The magnetic field causes a bias current and sense voltage on a nearby plate according to the Lorentz force. The closed-loop Hall effect sensor uses the bias current to sense wire current with high precision and resolution. Ultimately, this current is proportional to the current in the wire. (Crescentini et al. 2017).

The high-current measurement utilized the LEM LF_2010-S current transducer. With the current measurement resistor, this transducer allowed the data acquisition to measure ± 2000 A DC. The current range

specified encompassed the maximum value seen in previous testing. Additionally, the batteries were capable of outputting approximately 2000 CCA at 24°C (Trubac et al. 2022). As seen in in Figure 10, the 12.7 Ω resistor and the datasheet parameters were 0.2 mA/A secondary current sensitivity and 0.85 A maximum secondary current, allowing for a 2.54 mV/A sensitivity within the ±10 V DC NI 9229 range (LEM 2020).

Figure 10. DAQ high-current sensor schematic.

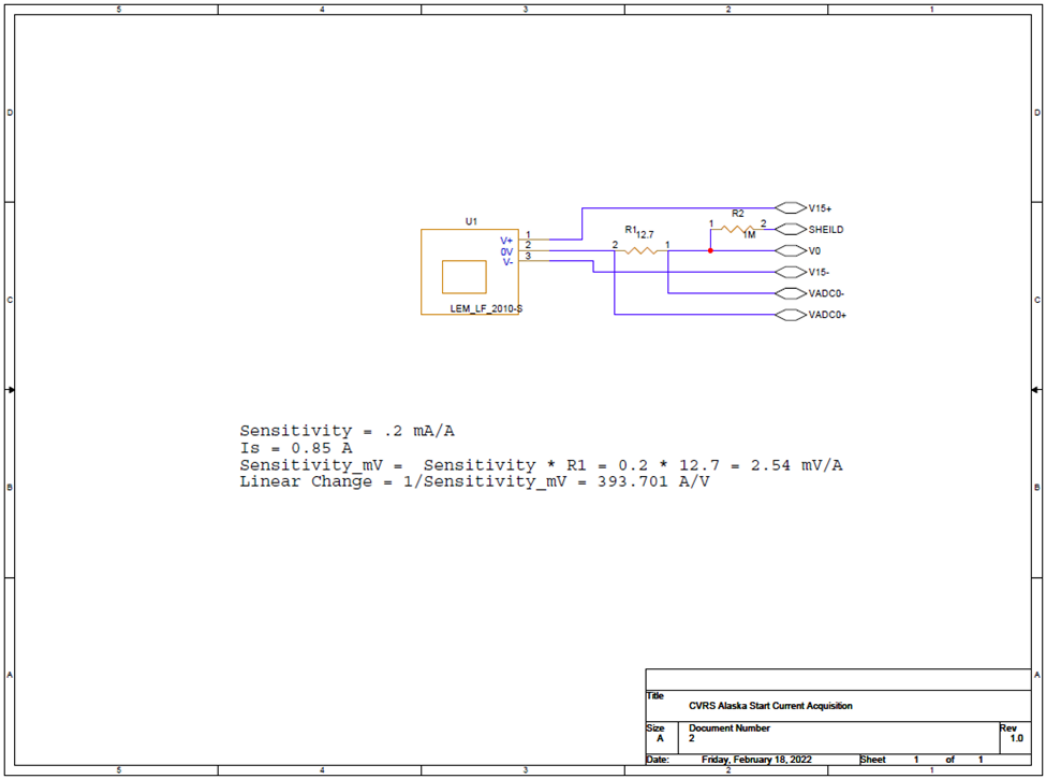

The low-current constant-draw testing used the CR Magnetics CR5210S-30 transducer. This transducer can measure ±30 A DC and output an analog voltage signal, within ±5 V, proportional to the current (CR Magnetics, n.d.). This voltage signal is directly readable by the NI 9220 voltage module.

This test needed to measure smaller currents as smaller currents can impede vehicle starting procedures by lowering battery capacity; these could range from tens of amps to milliamps, making the current resolution critical. Given the 6 A/V current sensitivity and 0.1526 mV/bit voltage resolution, the CR520S-30 has a resolution of 0.92 mA (CR Magnetics, n.d.). This fine resolution allowed the data acquisition to detect the smaller-problem currents mentioned. Figure 11 shows this setup.

Figure 11. DAQ low-current sensor schematic.

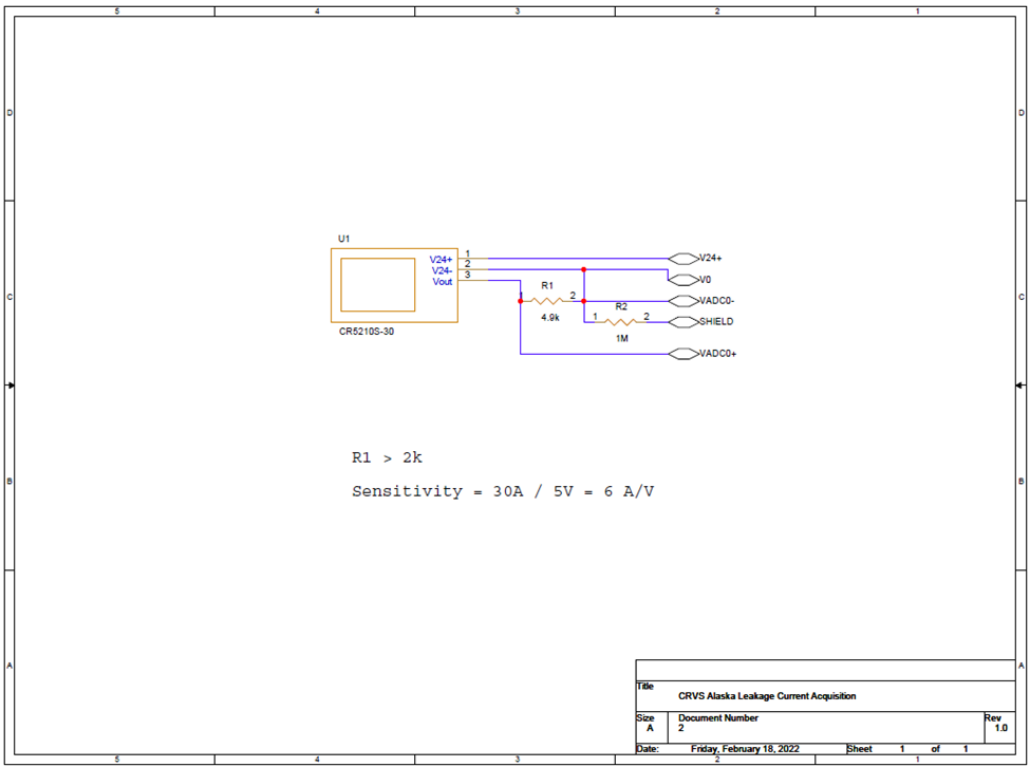

3.2.2.4 Temperature measurements

The NI 9212 thermocouple module allowed for measurement of all thermocouple types for a software-specified temperature range (NI 2021). All thermocouples were Type T, and the temperature range was set to –50°C to 100°C. Type T thermocouples can measure temperatures of –250°C to 400°C, which encompasses the expected range in Alaska (Dowell 2010).

3.2.2.5 Data acquisition software

There were two versions of this software—one for each type of test; both versions ran in NI LabVIEW. The software set the sample rate of the NI cDAQ-9178 and the NI module settings. For the CCA testing, the sample rate was set to 100 S/s to capture the short-duration event. Alternatively, the constant-draw software set the sample rate to 1 S/s due to the long duration. As mentioned above, all thermocouples were set to Type T, and all analog voltage measurements measure ±10 V DC. All data was converted to the proper units: degrees Celsius, volts, and amperes. Finally, all data was plotted.

Figure 12 shows the final construction of the DAQ system.

Figure 12. DAQ system for Alaska field testing.

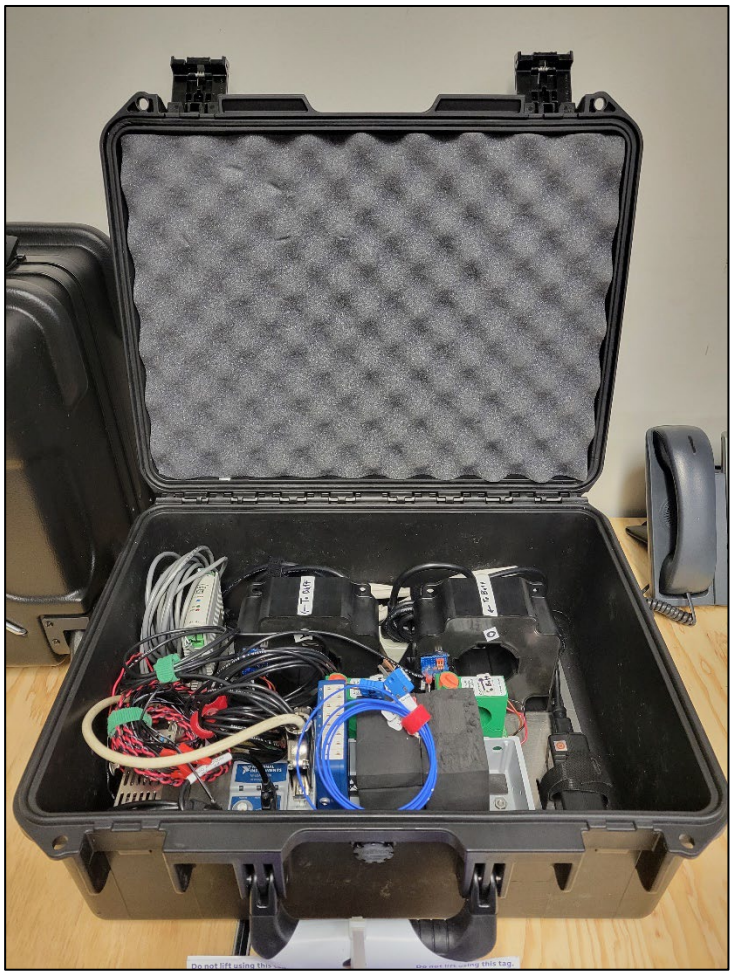

3.3 Test Procedure

The procedure established in Trubac et al. (2022) to evaluate the ultracapacitor modules was followed for this testing to evaluate the lithium-ion batteries. The same requirements applied to these tests: the batteries must successfully turnover the load system when set to the correct torque rating. A baseline was established at room temperature (28°C), and any unexpected variance from the results at the temperature would indicate if the batteries were affected by the decrease in temperature.

Again, the performance of the batteries was evaluated across the specified temperature range in Table 1. Once the batteries were fully charged, they were installed in the load system in CBx-21. The batteries were cold soaked for 24 hours to ensure all the components were at the desired temperature. Using the thermocouples installed on the system, testing was

initiated once all the temperature readings matched the ambient air-temperature measurement.

The procedure for this work varied from the previous procedure in that the batteries were tested by cranking the system at each temperature five times as opposed to three times. This was due to the increased capacity of the batteries compared to the ultracapacitor ESM's, meaning there was less depletion of the battery capacity by running the tests. The duration of the five tests was approximately 5 seconds, to stay consistent with the previous work. Once the five tests were complete at the specified temperature, the battery was removed and charged, then reinstalled into the load system. Once the battery was connected, the system was then brought down to the next temperature increment and cold soaked until the temperatures were consistent.

The procedure for the Alaska field tests followed a similar protocol to the previous phase and the cold room tests. Once the DAQ system was connected to the battery system, the vehicle was started three times. The duration of these tests was longer due to idling the vehicle so the batteries could be recharged by the alternator. Because the field tests were conducted in environmental conditions, there were no planned variations in temperatures between tests, just the natural changes in the ambient temperature. The vehicle was stored outside; and tests were conducted in the morning, then the vehicle and the batteries were left to cold soak at ambient air temperature until the next morning.

There also were several challenges encountered when collecting data on the Stryker battery system. Once of the main challenges was the very limited amount of space within the vehicle. This meant that the team had very little space to set up and install sensors and to work on equipment, which made it difficult to collect data on the necessary parts of the vehicle. Because of this, the battery box was very difficult to access in terms of data collection. The batteries that supplied power to the engine were not accessible with the DAQ sensors; however, the auxiliary batteries were. To gain any information on the Stryker system at all, the team installed the sensors on the auxiliary batteries, which captured the voltage draw of start-up, but the current draw was only what the auxiliary batteries experienced. The current draw on the auxiliary batteries during ignition followed the same trend as what the vehicle batteries would see, just at a much smaller magnitude, so the team determined it to be useful.

There were restrictions for photography of the Stryker and its battery system while on-base at Fort Wainwright, so no photos of the setup or the testing were taken. Section 3.2.2 describes the DAQ in detail in, and photos of a calibration test using a Polaris utility vehicle are discussed later in this report. The following section discusses all results obtained from these tests.

4 Results

4.1 CRREL cold room testing

Upon completion of the five tests at each temperature and then the following second round of five tests at each temperature (totalling ten tests per temperature), the team analyzed the data. The following sections discuss the resulting measurements for the torque of the system, speed of the flywheel, voltage at the battery, voltage at the starter motor, and current at the starter motor for the first round of the five tests at 28°C, 0°C, –20°C, and –40°C as well as the measurements for the second round of the five tests at 0°C and –40°C.

4.1.1 Data at 28 °C

At the ambient room temperature of the CRREL cold room complex (28°C), the battery was able to successfully start the mechanical load system for the five 5-second tests without failure. Figure 13 shows the results from the five tests at 28°C.

Figure 13 shows that the torque of the system (shown in blue) decreased after each of the five tests, starting at 324 N·m during the first test, which was the torque value the brake was set to. The torque then dropped to 290 N·m by the fifth test, a total drop of 33 N·m, yielding an average torque of 305 N·m for all five tests. The speed of the flywheel (shown in red) stayed consistent, averaging 443 rpm for all five tests. Table 4 shows averages, which were calculated using MATLAB, of the flywheel speeds and torques of each test during steady state.

The consistency of the flywheel speed between the five tests is likely because the voltage of the battery stayed at relatively the same value after each test (Figure 14).

Figure 14 shows that the voltage of the battery dropped approximately 8 V upon initiation of each test. Test 1 started with a voltage of 30 V, spiked down to 22.5 V, rose to 27.5 V during the test, and then returned to 30 V upon completion of the test. The subsequent tests followed the same trend, starting around 30 V, spiking down to between 22 V and 23 V, rising to 27 V–28 V during the 5-second tests, and then returning 29 V–30 V upon completion.

Figure 13. Measurements of torque, flywheel speed, and starter current from all five tests at 28°C.

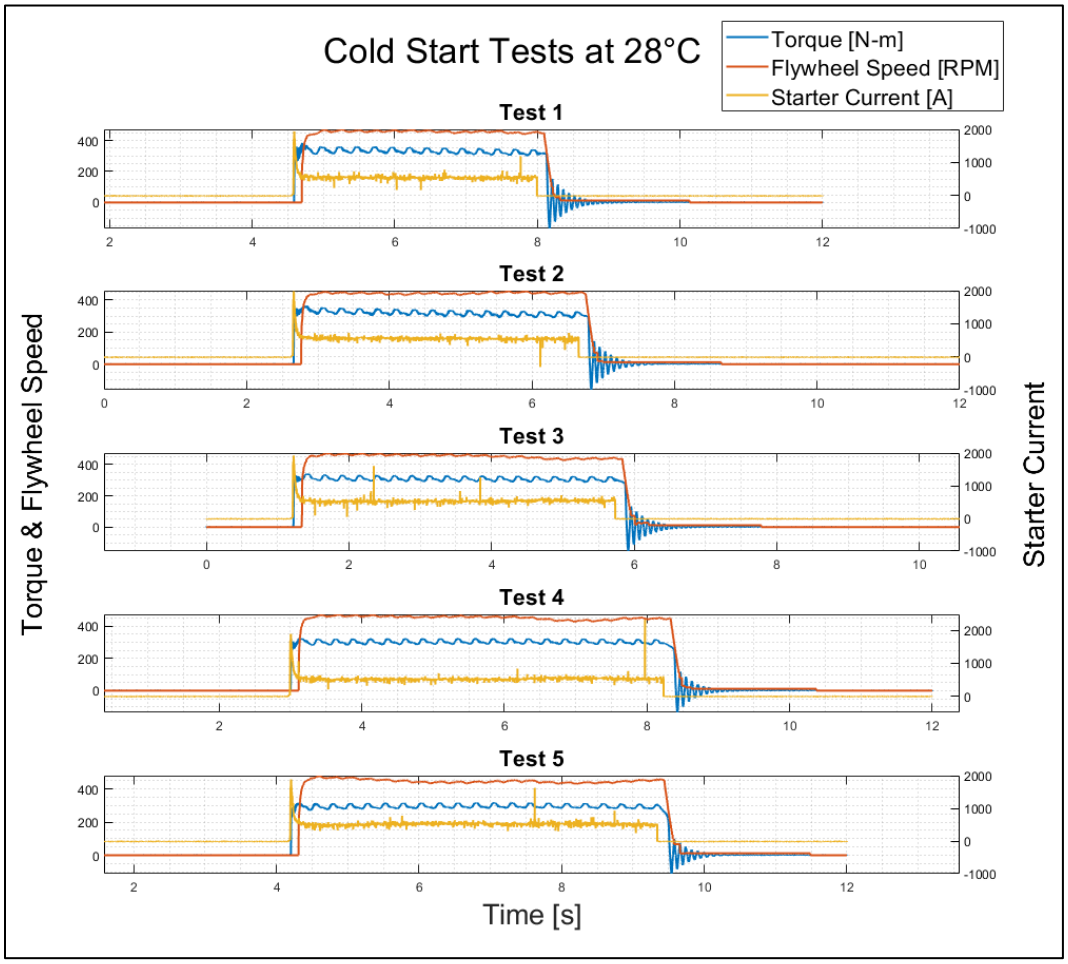

Table 4. Calculated average flywheel speed and torque values for all five 28°C tests.

Test #	Average Speed (rpm)	Average Torque (N · m)
1	447.15	323.50
2	436.28	313.18
3	445.71	302.48
4	447.18	297.68
5	441.99	290.39
Average of all five tests	443.66	305.44

Figure 14. Voltages of the battery for all five tests at 28°C.

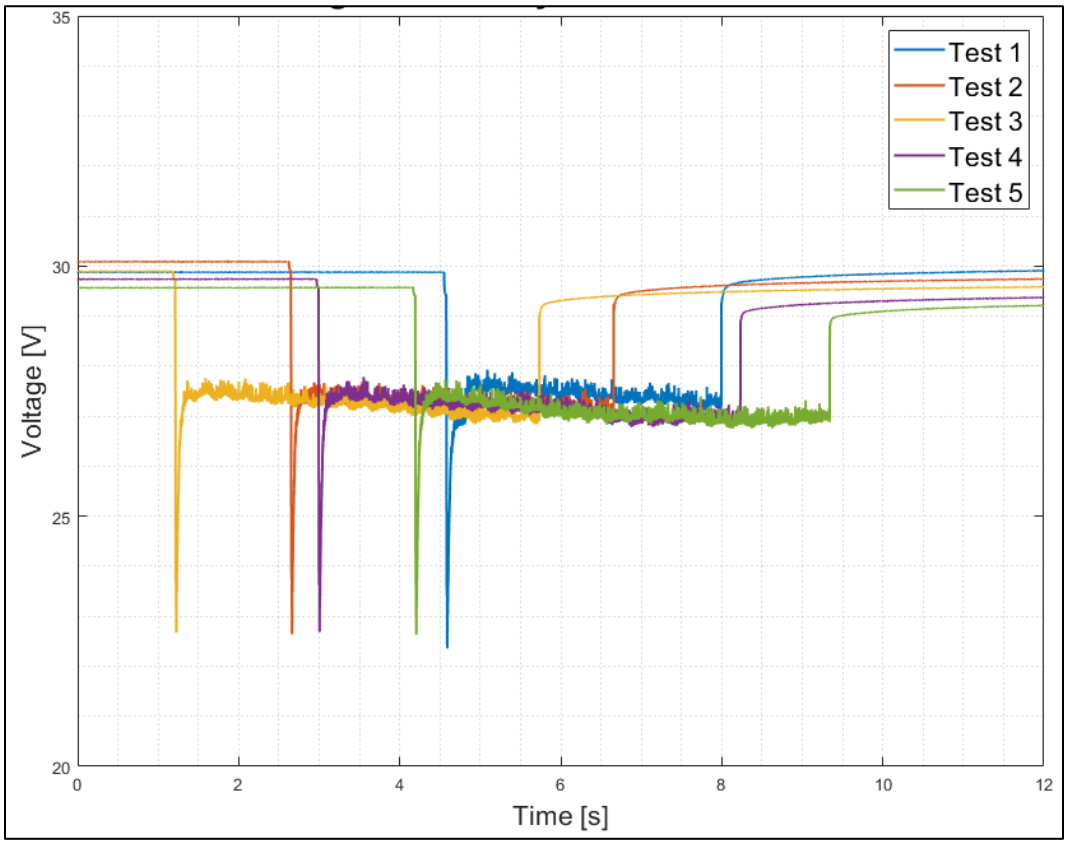

These tests at 28°C acted as a baseline to compare how the cold impacts performance of the battery. If any parameters changed, it indicated that the battery was affected by cold environments to some extent.

4.1.2 Data at 0°C

There is very little difference between the tests at 28°C and the tests run at 0°C. Figure 15 shows the resulting measurements.

In Figure 15, the only noticeable difference between the tests at 0°C and the 28°C tests is the speed of the flywheel. While the 28°C tests held an average of 443 rpm for all five tests, the speed of the flywheel for all five of the 0°C tests averaged 410 rpm. The torque stayed consistent between the 28°C and 0°C tests, at an average of 324 N·m for all five tests. The torque still decreased after each of the tests, similar to the 28°C tests but to less of an extent. There was a 25 N·m drop between the first and fifth tests at 0°C compared to the 33 N·m drop between the first and fifth tests at 28°C. Table 5 shows the averages, calculated using MATLAB, of the flywheel speeds and torques of each test during steady-state.

Figure 15. Measurements of torque, flywheel speed, and starter current from all five tests at 0°C.

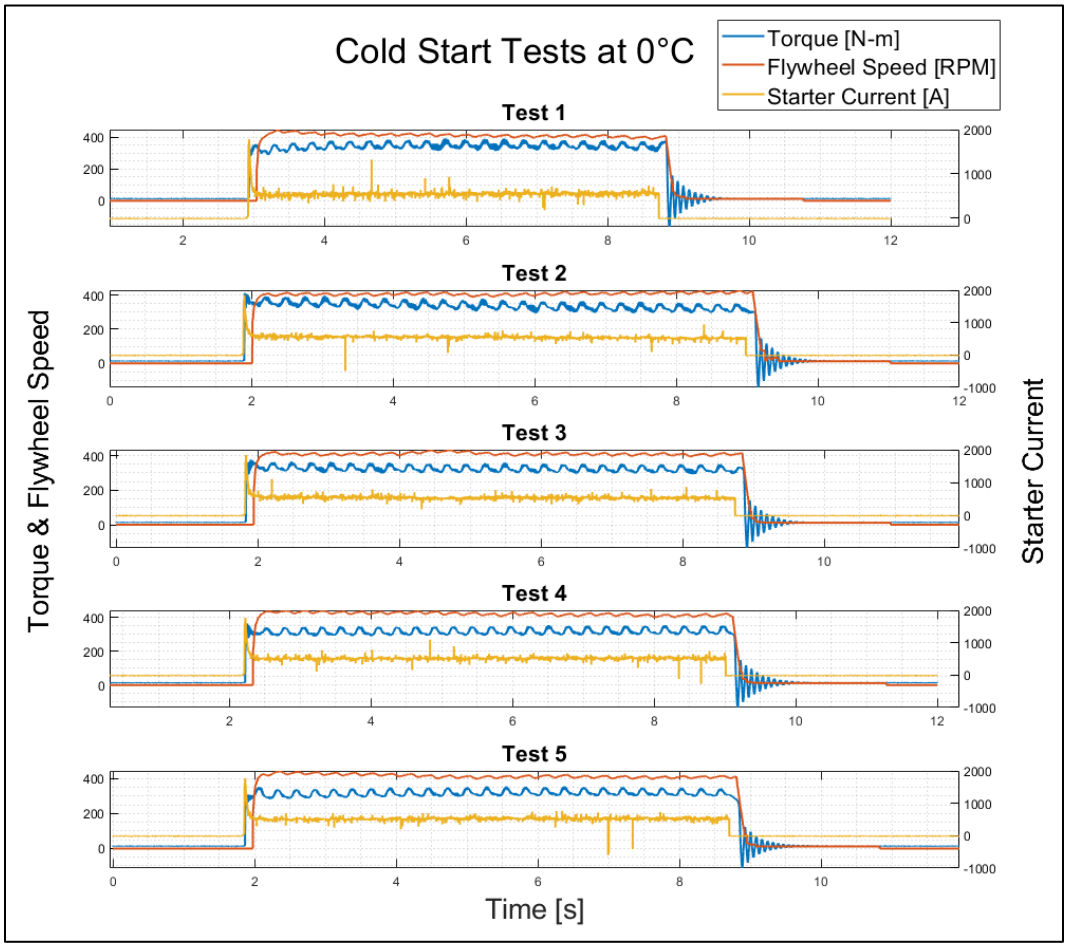

Table 5. Calculated average flywheel speed and torque values for all five 0°C tests.

Test #	Average Speed (rpm)	Average Torque (N·m)
1	408.80	339.70
2	404.27	332.94
3	407.41	320.50
4	416.94	312.72
5	412.06	313.85
Average of all five tests	409.89	323.94

There is minimal difference between the 0°C tests and the 28°C tests, which comparing the voltages of the five 0°C tests to each other shows (Figure 16).

Figure 16. Voltages of the battery for all five tests at 0°C.

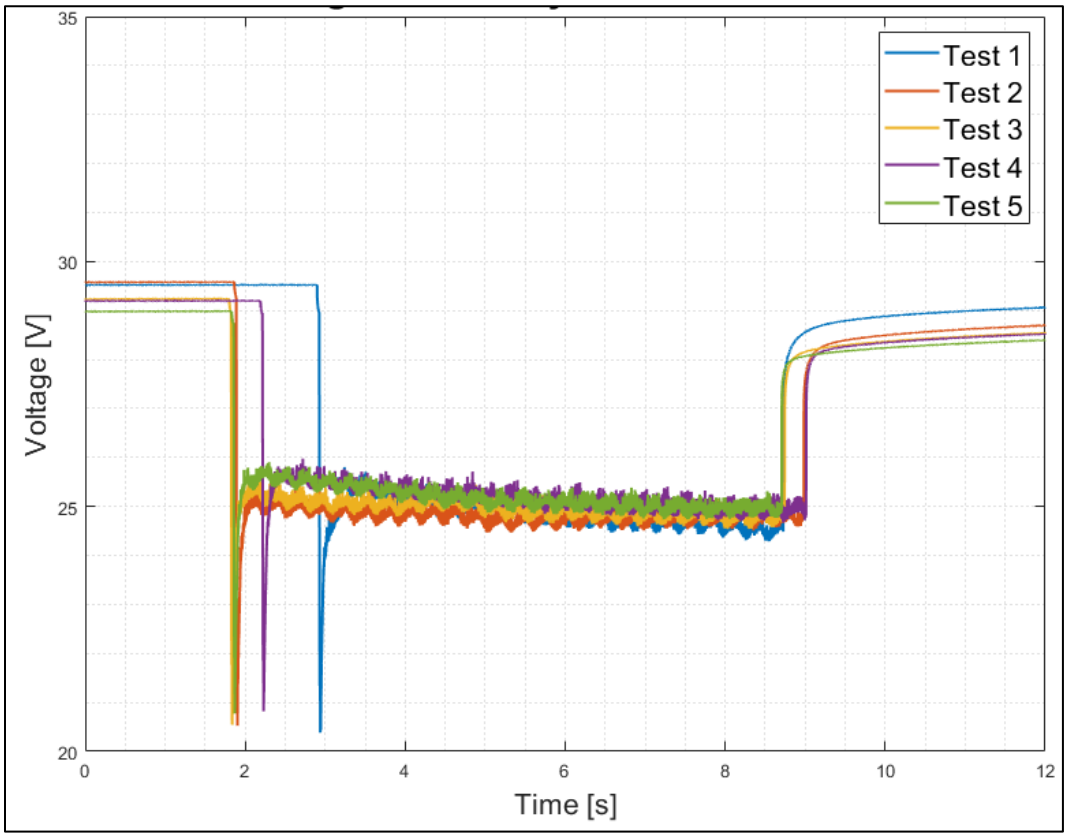

Figure 16 shows that the differences between spike down of the voltages of the five tests at 0°C (9 V) are greater than the spike down of the three voltages at 28°C (8 V), but only slightly. The 0°C tests followed the same trend as the 28°C tests and had very similar values for the voltages.

Figure 16 shows that the voltage of the battery dropped approximately 9 V upon initiation of each test. Test 1 started with a voltage of 29.5 V, spiked down to 20.5 V, rose to 25 V during the test, and then returned to 29 V upon completion of the test. The subsequent tests followed the same trend, starting around 29 V–30 V, spiking down to between 20 V and 21 V, rising to 24 V–26 V during the 5-second tests, and then returning to 28 V–29 V upon completion.

4.1.3 Data at −20°C

Again, there is very little difference between the tests at 28°C and 0°C and the −20°C tests. All five of the 5-second tests were still able to be achieved during the −20°C tests; Figure 17 illustrates these.

Figure 17. Measurements of torque, flywheel speed, and starter current from all five tests at −20°C.

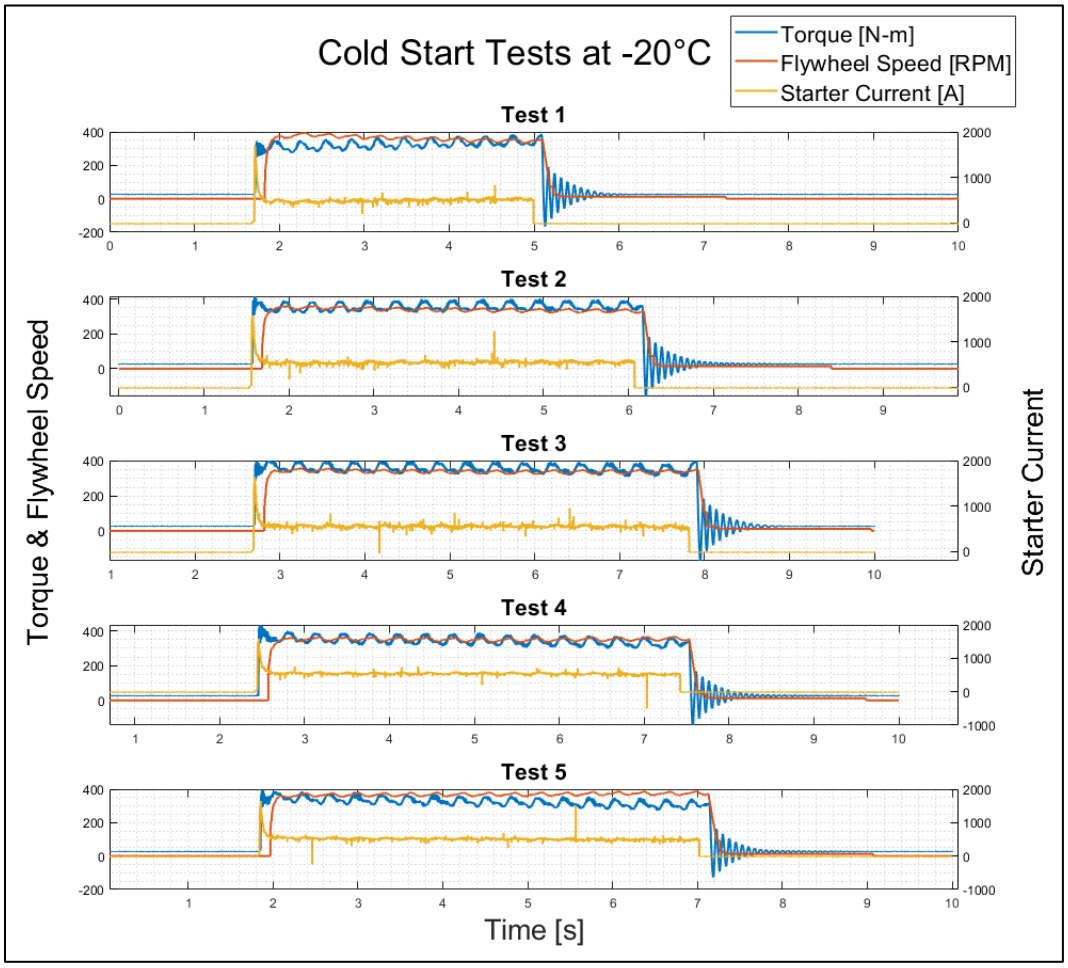

When comparing the tests conducted at −20°C to the 28°C and 0°C tests, again, the speed of the flywheel is the only notable difference between them. While the 28°C tests held an average of 443 rpm for all five tests and 410 rpm for all five of the 0°C tests, the speed of the flywheel averaged 348 rpm for the five −20°C. The torque still decreased after each of the −20°C tests, similar to the 28°C and 0°C tests. There was a 29 N·m drop between the second and fifth tests at −20°C, compared to the 33 N·m drop between the first and fifth tests at 28°C and the 25 N·m drop between the first and fifth tests at 0°C. The torque of the first test was 318 N·m, which then jumped up to 350N·m for the second test; the cause is unknown.

Table 6 shows averages, calculated using MATLAB, of the flywheel speeds and torques of each test during steady state.

Table 6. Calculated average flywheel speed and torque values for all five −20°C tests.

Test #	Average Speed (rpm)	Average Torque (N · m)
1	357.03	318.48
2	336.50	350.04
3	335.96	350.54
4	346.90	337.82
5	365.36	320.25
Average of all five tests	348.35	335.43

The differences in the voltages of the 28°C tests and the 0°C tests are relatively small; Figure 18 shows a similar trend for the five −20°C tests.

Figure 18. Voltages of the battery for all five tests at −20°C.

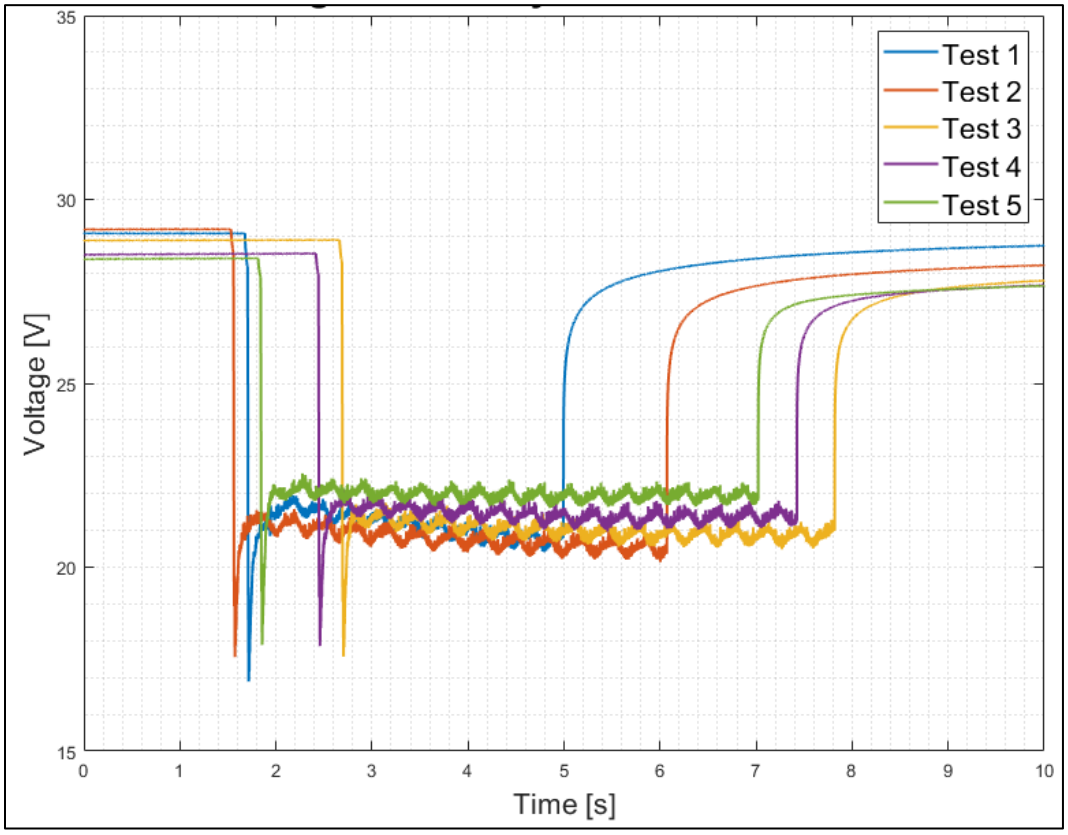

Figure 18 shows that the differences between the spike down of the voltages of the five tests at −20°C (12 V) were greater than the spike down of the five voltages at 0°C (9 V) and spike down of the five tests at 28°C (8 V). The −20°C tests followed the same trend as the 0°C and 28°C tests and had very similar values for the voltages. The voltage of the battery dropped

approximately 12 V upon initiation of each test. Test 1 started with a voltage of 29.25 V, spiked down to 17 V, rose to 21.5 V during the test, and then returned to 29 V upon completion of the test. The subsequent tests follow the same trend, starting around 28 V–29 V, spiking down to between 17 V and 18 V, rising to 20 V–22 V during the 5-second tests, and then returning to 28 V–29 V upon completion.

4.1.4 Data at −40°C

Prior to the tests at −40°C, there was an issue encountered when testing at −30°C. After cold soaking the battery at −30°C, the battery was not starting the system initially. No energy was being discharged to turn over the system. The battery was removed from the cold room and brought to room temperature. It was determined the electronics had deactivated the battery due to low temperatures and were not letting the battery discharge. The battery was then reactivated and left to cold soak again at −30°C to attempt to repeat the tests, but it yielded the same result. It was determined that the battery will deactivate itself once it reaches an internal temperature of −20°C, so as not to damage the battery components. When operating below −20°C, an internal heater needs to be activated. To do so, the battery needs to be connected to the battery management program via the communications cable. This presents a challenge as the batteries would not be constantly connected to the battery management program while installed in a Stryker. To see if the internal heater could be enabled by only having the cable connected to the communication port on the battery but not connected to the program, the battery was left to cold soak at −30°C again with just the communications cable connected. It was determined that this was not a solution as the battery deactivated again.

Since this evaluation intended to replicate the Stryker vehicle battery system, it was not practical for the battery to need to be connected to the management program while operating.

4.2 Alaska field testing

4.2.1 Calibration vehicle tests

To verify that the portable DAQ system was functioning correctly, it was connected to a Polaris Utility Vehicle at the CRREL Alaska Research Office site (Figure 19). Several room-temperature calibration tests were

conducted to ensure all sensors were operating and the data was being logged correctly.

Figure 19. Polaris utility vehicle used for DAQ system calibration.

Each set of sensors was tested separately since the Polaris only had one 12 V lead-acid battery. The current transducer was connected around the positive battery cable running to the engine, and the voltage sensor was connected to the positive and negative terminals of the battery, shown in Figure 20.

Figure 20. Polaris battery configuration.

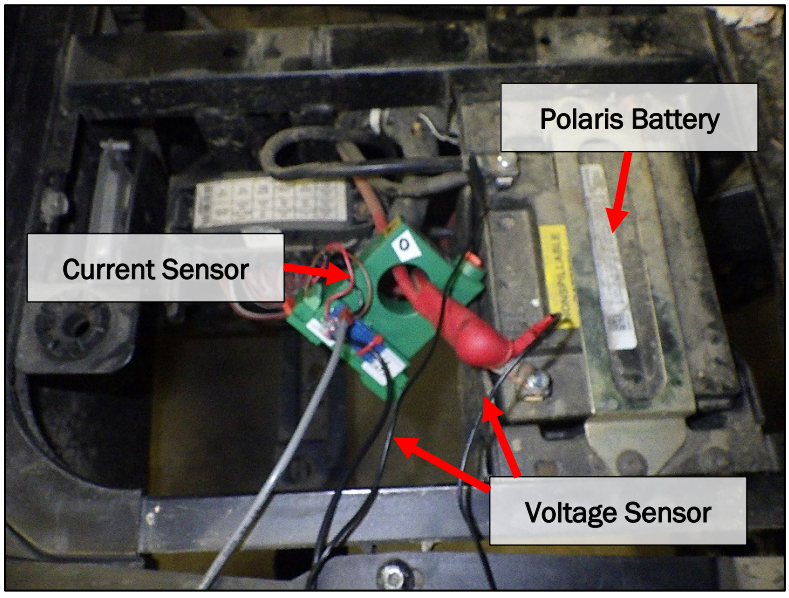

Figure 21 shows the voltage and current measurements collected from the Polaris using the DAQ.

Figure 21. Voltage and current measurements collected from the Polaris.

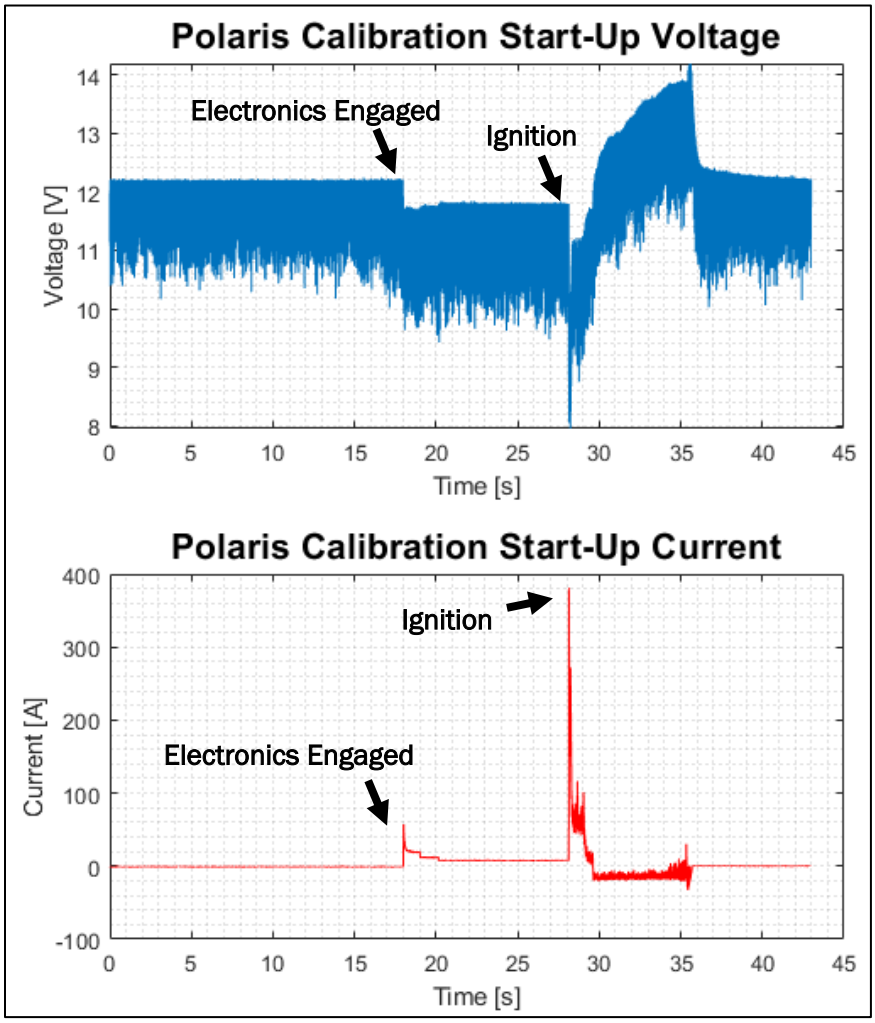

Figure 21 shows that the DAQ operated correctly and registered the proper trends for vehicle start. The voltage results show that without any electronics active, the battery read 12.2 V, then once the electronics were activated, the voltage read 11.8. Upon start-up of the engine, the voltage dropped to approximately 9.5 V, where it then gradually increased as the alternator recharged the system. The voltage returned to 12.2 V once the engine was turned off. There was some noise in the voltage signal, but it is unclear as to the cause as it occurred with only the Polaris. The current has a small spike of 57.3 A when the electronics were engaged, then a small draw of 8.2 A until the starter was engaged, which was a much larger spike of 380.8 A. The current then dropped during idle and returned to 0 A once the engine was shut off. The black arrows indicate when in the data the electronics were engaged and when ignition occurred.

These results indicate that the DAQ system was functioning correctly and was able to capture the necessary trends.

4.2.2 Stryker battery system tests

All the tests with the 12 V lead-acid Hawker batteries in the Stryker were conducted at the ambient air temperature in Fairbanks, Alaska, 14–18 March. Figure 22 shows the temperatures of each battery and the ambient air for Tests 1, 2, and 3.

Figure 22. All temperatures for Tests 1, 2, and 3.

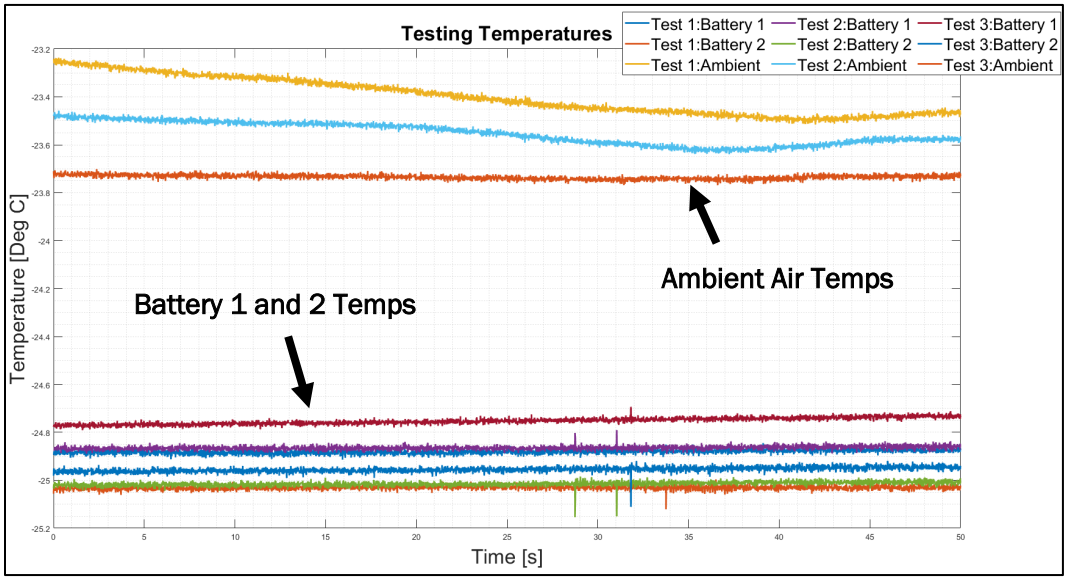

Figure 22 shows that for all three tests, the ambient air temperature was slightly higher than the two battery temperatures. Table 7 shows the average temperatures for all three tests.

Table 7. Average temperatures for Tests 1, 2, and 3.

Test #	Ambient Temperature	Battery 1 Temperature	Battery 2 Temperature
1	−23.40°C	−24.88°C	−25.03°C
2	−23.55°C	−24.86°C	−25.01°C
3	−23.73°C	−24.75°C	−24.96°C
Average of all three tests	−23.56°C	−24.83°C	−25.00°C

The 1.36°C difference between the ambient air temperature and the average temperature of both batteries is likely because the ambient air temperature changed faster than the battery temperature as it got later in the day since the batteries hold their temperature better than the air.

The start-up procedure for a Stryker involves two stages: electrical component activation, then engine ignition. Figure 23 shows the voltage and current for the first test.

Figure 23. Stryker battery Test 1 voltage and current.

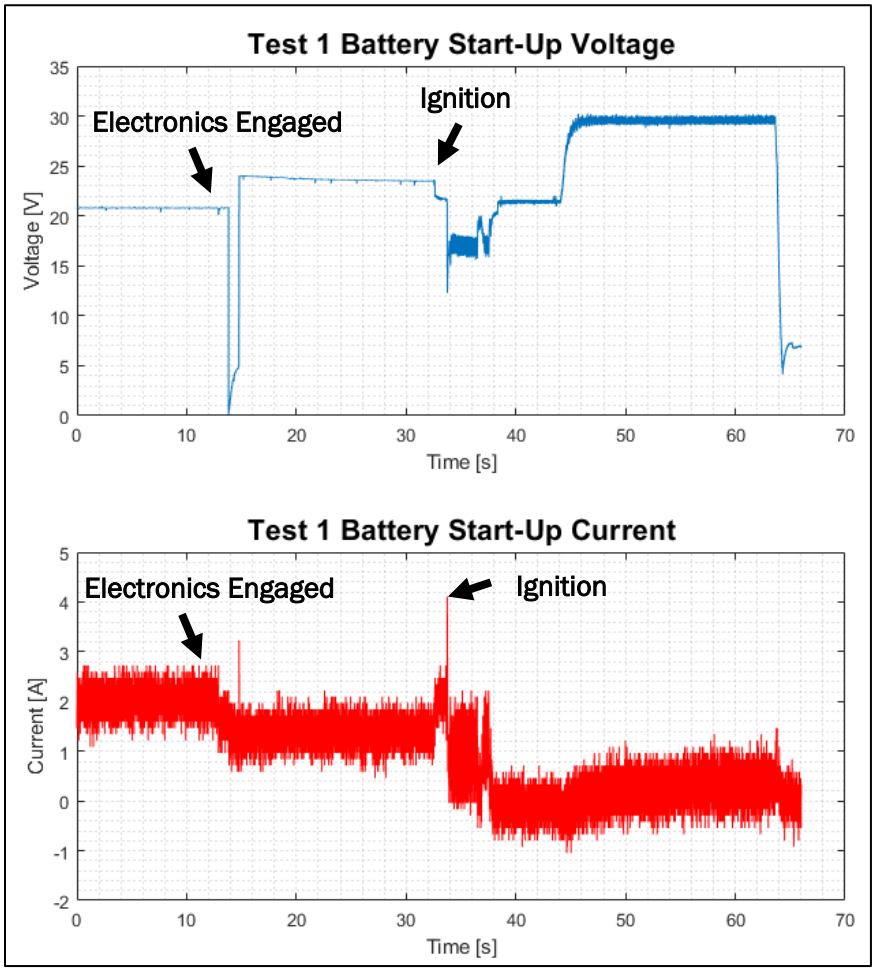

Figure 23 shows an initial voltage of 20.8 V, where it then drops almost down to 0 V when the electronics are engaged, and then another drop to approximately 17.5 V when the engine is cranking. The voltage then increases to 29.5 V once the vehicle has started and the alternator is recharging the batteries. The same trend can be seen in the current, with an initial spike when the electronics engage and then again when the engine is cranking. However, since the data was collected on the auxiliary batteries,

not the vehicle batteries, the values of the current are much lower than what the vehicle batteries would experience. This trend was the same for all three tests run with the Stryker battery system, and all the values were consistent (Figure 24 and Figure 25).

Figure 24. Stryker battery Test 2 voltage and current.

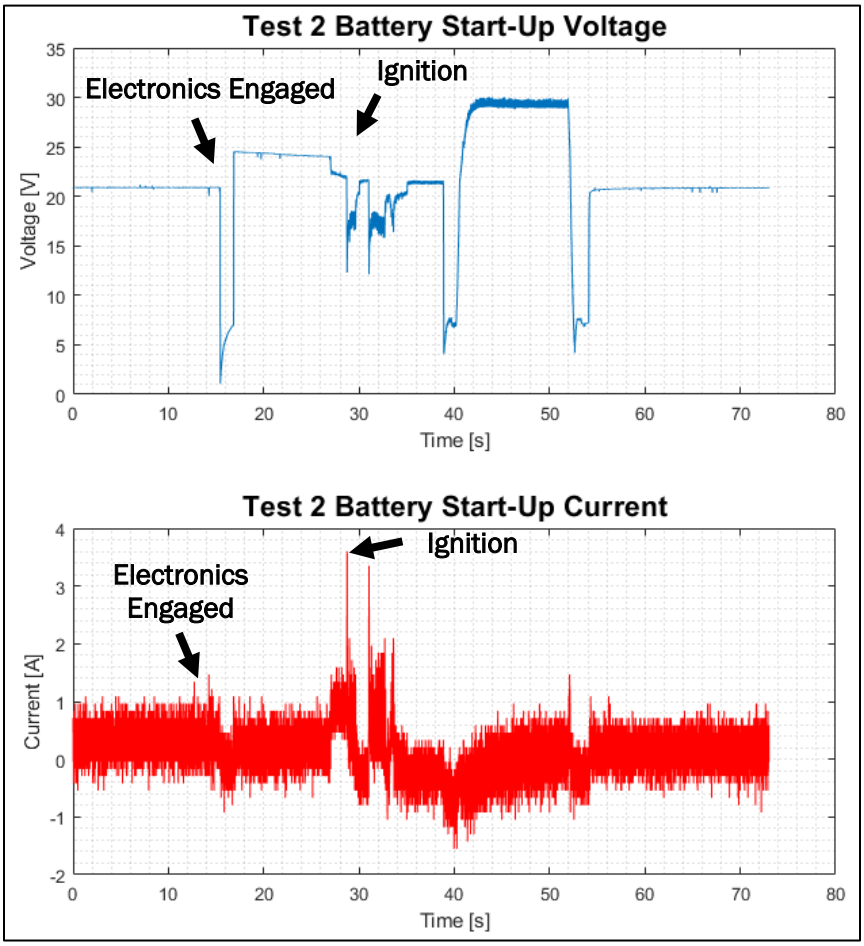

Figure 24 also shows an initial voltage of 20.8 V, a drop almost down to 0 V when the electronics are engaged, and then another drop to approximately 17.3 V when the engine is cranking. The voltage then increases to 29.3 V once the vehicle has started and the alternator is recharging the batteries. The same trend can be seen in the current, with an initial spike when the electronics engage and then again when the engine is cranking.

Test 3 has this pattern also. Figure 25 shows an initial voltage of 20.8 V, a drop almost down to 0 V when the electronics are engaged, and then another drop to approximately 19.2 V when the engine is cranking. The voltage then increases to 29.5 V once the vehicle has started and the alternator

is recharging the batteries. The current for Test 3 does not show as clear an indication of the trend as Tests 1 and 2, so the engagement of the electronics and the ignition are not as noticeable. There is more noise in Test 3, but the cause is unclear.

Figure 25. Stryker battery Test 3 voltage and current.

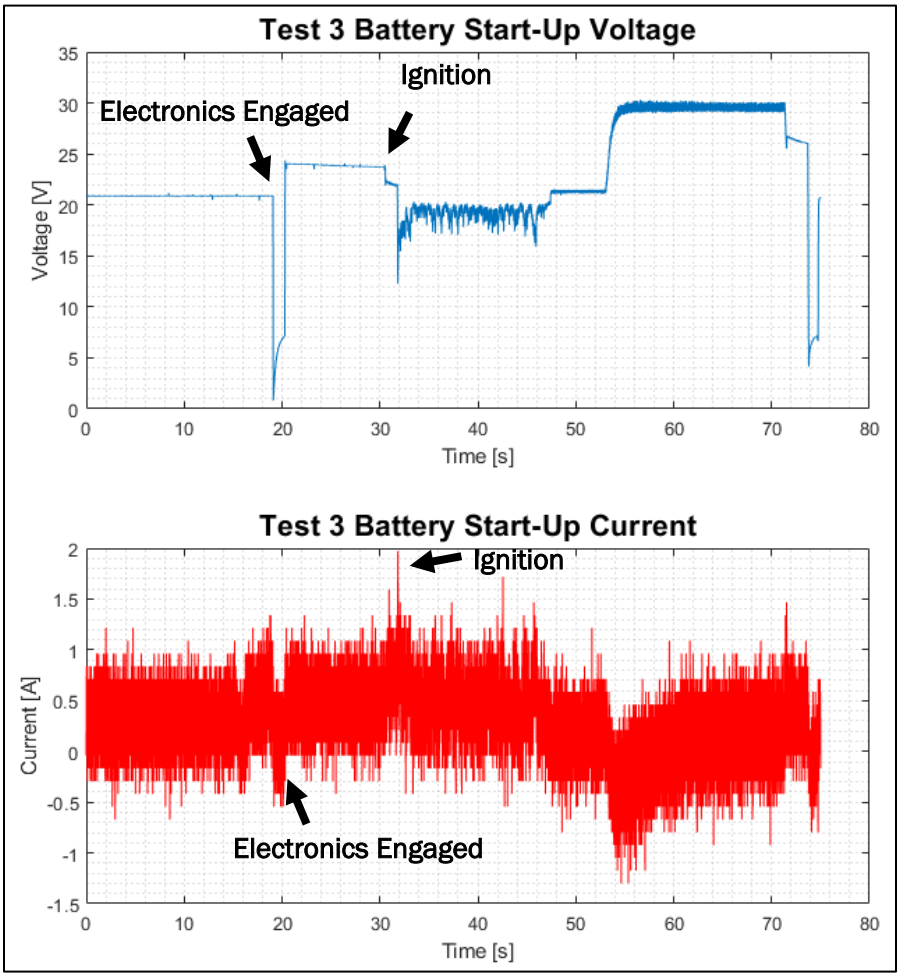

4.3 Discussion

Upon completion of the cold room testing, the team determined that the performance of the battery was not significantly affected by temperature. There was very little impact on the voltage used to run the five tests at each temperature; and the current, flywheel rpm, and torque were all consistent across the five tests at each temperature. There was some variation of those parameters as the temperature decreased, but those differences can be attributed to the increased resistance the load system encounters as the temperature decreases. As the system got colder, the mechanical compo-

nents of the load system became increasingly more difficult to engage, either from the bearings being cold and increasing the resistance or the starter motor potentially being affected by the cold and not operating as effectively. This is a very realistic scenario that a vehicle operating in cold regions could encounter, since batteries are not the only components that would be impacted by the cold. As temperatures drop, oils, greases, and other fluids in the engine and the vehicle itself will be impacted and may not operate to their original capacity.

However, the internal heater needing to be activated for the battery to operate below –20°C poses a challenge for operating this technology in a Stryker in the field. From the information gained during the Alaska field testing with the 1-25th Stryker Brigade, the batteries would not be constantly connected to a communications cable during vehicle operation, so it would not be possible to activate the internal heater when temperatures reach –20°C and below.

After completing the Stryker battery testing, the team more thoroughly understood the existing battery system of the Stryker. Significant space restrictions in the vehicle, including the battery box, made it very difficult to instrument the batteries with the DAQ system. However, the data collected showed the voltage requirements any battery technology would need to meet to operate the system.

5 Conclusions

Operating heavy-duty military vehicles in cold regions continues to pose challenges, both from a starting-capability standpoint and mobility standpoint. Next-generation battery technology used to start large diesel engines could possibly improve this. Therefore, this work focused on improving vehicle cold-start capabilities of Stryker Combat Vehicles by characterizing the existing Stryker battery system in the cold and then evaluating the performance of the Bren-Tronics Inc. Brenergy BT-70939M-TPA/-TPB: 6T 24 V High-Power Li-Ion Battery at various temperatures. Using a simulated mechanical load system developed in a previous study, the team evaluated the battery across a series of temperatures ranging from 28°C to –40°C. Additionally, the Stryker battery system was evaluated using a mobile DAQ system at –25°C during field testing at Fort Wainwright in March.

The results obtained from these tests show that the battery proved capable of turning over the simulated engine down to –20°C with no noticeable changes but encountered issues related to the internal heater component and the battery management program at temperatures below –20°C. The team determined that it was impractical to have the batteries constantly connected to the battery management system when operating the vehicle for temperatures below –20°C. It was also discovered that the cold impacted the simulated load system, similar to what a real engine system would experience as the testing temperatures decreased. Additionally, the Stryker battery system has significant space constraints, which limited the data that could be collected on the system. However, despite the space constraints, the voltage measurements collected from the batteries during start-up clearly showed the requirements the batteries are designed to meet. Due to the measurements being taken on the auxiliary batteries verses the vehicle batteries, the current measurements were not of the same magnitude as they would be for the vehicle batteries, but the trend was still consistent.

With the information gained from this work, the next steps in investigating cold-capable start technology would be to further investigate this battery technology at the lower temperature range to overcome the challenges encountered in this study. Additionally, it would be useful to investigate next-generation lithium-ion battery technologies for additional vehicle

platforms. Now that the Stryker system is more fully understood, the battery technology could be adapted for use in many different vehicle platforms, and the improvements documented in this report could be leveraged for other cold-related applications.

References

Alaska Department of Labor and Workforce Development. 2020. *Alaska Population Overview: 2019 Estimates*. Juneau, AK: Department of Labor and Workforce Development. https://live.laborstats.alaska.gov//pop/estimates/pub/19popover.pdf.

Battery University. 2021. "BU-205: Types of Lithium-Ion." Battery University. Last modified 11 February 2021. https://batteryuniversity.com/index.php/learn/article/types_of_lithium_ion.

Battle Born Batteries. 2020. *Lead is Dead: Cold Charging LFP vs Lead Acid*. Reno, NV: Battle Born Batteries. https://battlebornbatteries.com/wp-content/uploads/2020/10/Lead-is-Dead-Cold-Charging-LFP-vs-Lead-Acid.pdf.

Berrueta, A., A. Ursua, I. S. Matin, A. Eftekhari, and P. Sanchis. 2019. "Supercapacitors: Electrical Characteristics, Modeling, Applications, and Future Trends." *IEEE Access* 7: 50869–50896. https://doi.org/10.1109/ACCESS.2019.2908558.

Bukhari, S. M. A. S., J. Maqsood, M. Q. Baig, S. Ashraf, and T. A. Khan. 2015. "Comparison of Characteristics - Lead Acid, Nickel Based, Lead Crystal and Lithium Based Batteries." In *2015 17th UKSim-AMSS International Conference on Modelling and Simulation (UKSim)*, 25–27 March, Cambridge, UK, 444–450. https://doi.org/10.1109/UKSim.2015.69.

Cowie, I. 2015. "All About Batteries, Part 12: Lithium Titanate (LTO)." *EE Times*, 21 January 2015. https://www.eetimes.com/all-about-batteries-part-12-lithium-titanate-lto/#.

CR Magnetics. n.d. *DC Current Transducer: Din Rail/Panel Mount*. Accessed 12 May 2022. St. Louis, MO: CR Magnetics. https://www.crmagnetics.com/Assets/ProductPDFs/CR5200%20Series%20Catalog%20Page.pdf.

Crescentini, M., S. F. Syeda, and G. P. Gibiino. 2017. "Hall-Effect Current Sensors: Principles of Operation and Implementation Techniques." *IEEE Sensors Journal* 22 (11): 10137–10151. https://doi.org/10.1109/JSEN.2021.3119766.

Dowell, D. L. D. 2010. "A Critical Look at Type T Thermocouples in Low-Temperature Measurement Applications." *International Journal of Thermophysics* 31:1527–1532. https://doi.org/10.1007/s10765-010-0780-2.

Hutchinson, R. 2004. *Temperature Effects on Sealed Lead Acid Batteries and Charging Techniques to Prolong Cycle Life*. SAND2004-3149. Albuquerque, NM: Sandia National Laboratories. https://doi.org/10.2172/975252.

Jaguemont, J., L. Boulon, Y. Dube, and D. Poudrier. 2015. "Low Temperature Discharge Cycle Tests for a Lithium Ion Cell." In *2014 IEEE Vehicle Power and Propulsion Conference*, 27–30 October 2014, Coimbra, Portugal. https://doi.org/10.1109/VPPC.2014.7007097.

Lam, M. 2020. "A $LiFePO_4$ Battery vs Lithium Ion Polymer Battery." *Medium*, 9 June 2020. https://medium.com/battery-lab/a-lifepo4-battery-vs-lithium-ion-polymer-battery-6a028111efa3.

LEM. 2020. *Current Transducer LF 2010-S*. Version 3. https://www.lem.com/sites/default/files/products_datasheets/lf_2010-s.pdf.

Li, J., Z.-F. Ma. 2019. "Past and Present of $LiFePO_4$: From Fundamental Research to Industrial Applications." *Chem* 5(1): 3–6. https://doi.org/10.1016/j.chempr.2018.12.012.

Liu, H., Z. Wang, J. Cheng, and D. Maly. 2009. "Improvement on the Cold Cranking Capacity of Commercial Vehicle by Using Ultracapacitor and Lead-Acid Battery Hybrid." *IEEE Transactions on Vehicular Technology*. 58 (3): 1097–1105. https://doi.org/10.1109/TVT.2008.929220.

NATO. 2017. *Standardization of Electrical Systems in Tactical Land Vehicles*. STANAG 2601. Brussels, Belgium: NATO.

NI (National Instruments). 2022. *NI 9220 Getting Started*. Austin, TX: National Instruments. https://www.ni.com/pdf/manuals/373920f.pdf.

NI (National Instruments). 2021. "NI-9212 Specifications." National Instruments. Last modified 18 December 2021. https://www.ni.com/docs/en-US/bundle/ni-9212-specs/page/specifications.html.

NI (National Instruments). 2016. *NI cDAQTM-9171/9174/9178 User Manual: NI Compact-DAQ USB 2.0 Chassis*. Austin, TX: National Instruments. https://www.ni.com/pdf/manuals/372838e.pdf.

Satyavani, T., A. Kumar, P. Rao. 2016. "Methods of Synthesis and Performance Improvement of Lithium Iron Phosphate for High Rate Li-Ion Batteries: A Review." *Engineering Science and Technology, an International Journal* 19 (1): 178–188. https://doi.org/10.1016/j.jestch.2015.06.002.

Shao-Horn, Y., L. Croguennec, C. Delmas, E. C. Nelson, M. A. O'Keefe. 2003. "Atomic Resolution of Lithium Ions in $LiCoO_2$." *Nature Materials* 2:464–467. https://doi.org/10.1038/nmat922.

TARDEC (US Army Tank-Automotive Research, Development, and Engineering Center). 2019. *Performance Specification: Battery, Rechargeable, Sealed, 6T Lithium-Ion*. MIL-PRF-32565B. Warren, MI: Department of Defense, TARDEC.

Trubac, K., C. Callaghan, C. Hartshorn, T. Elliot, D. Punt, and C. Donnelly. 2022. *Cold Regions Vehicle Start: Cold Performance of Ultracapacitor-Based Batteries for Stryker Vehicles*. ERDC/CRREL TR-22-20. Hanover, NH: US Army Engineer Research and Development Center, Cold Regions Research and Engineering Laboratory.

University of Texas at Austin. 2020. "New Cobalt-Free Lithium-Ion Battery Reduces Costs without Sacrificing Performance." *ScienceDaily*, 16 July 2020. www.sciencedaily.com/releases/2020/07/200716101612.htm.

US Army Alaska. 2020. "U.S. Army Alaska | Units." U.S. Army Alaska. Last modified 7 April 2020. https://home.army.mil/alaska/index.php/USARAK-units.

Wang, L., Z. Wang, Q. Ju, W. Wang, Z. Wang. 2017. "Characteristic Analysis of Lithium Titanate Battery." *Energy Procedia* 105:4444–4449. https://doi.org/10.1016/j.egypro.2017.03.942.

Abbreviations

AC	Alternating current
CAN	Controller area network
CCA	Cold-cranking amps
CRREL	Cold Regions Research and Engineering Laboratory
DAQ	Data acquisition
DC	Direct current
ERDC	Engineer Research and Development Center
ESM	Engine start module
LCO	Lithium cobalt oxide
$LiCoO_2$	Lithium cobalt oxide
$LiFePO_4$	Lithium iron phosphate
Li-ion	Lithium-ion
$LiTiO_3$	Lithium titanate
NI	National Instruments
SBCT	Stryker Brigade Combat Team

REPORT DOCUMENTATION PAGE

Form Approved

OMB No. 0704-0188

1. REPORT DATE (DD-MM-YYYY)	2. REPORT TYPE	3. DATES COVERED (From - To)
November 2022	Final Technical Report (TR)	FY21–FY22

4. TITLE AND SUBTITLE

Cold Regions Vehicle Start: Next-Generation Lithium-Ion Battery Technologies for Stryker Vehicles

5a. CONTRACT NUMBER

5b. GRANT NUMBER

5c. PROGRAM ELEMENT

0603119A

6. AUTHOR(S)

Kathryn P. Trubac, Randall W. Reynolds, Timothy J. Cooke, Caylin A. Hartshorn, Douglas A. Punt, Christopher J. Donnelly, and Caitlin A. Callaghan

5d. PROJECT NUMBER

B03

5e. TASK NUMBER

SBO307 and SBO348

5f. WORK UNIT NUMBER

7. PERFORMING ORGANIZATION NAME(S) AND ADDRESS(ES)

US Army Engineer Research and Development Center (ERDC)
Cold Regions Research and Engineering Laboratory (CRREL)
72 Lyme Road
Hanover, NH 03755-1290

8. PERFORMING ORGANIZATION REPORT NUMBER

ERDC/CRREL TR-22-23

9. SPONSORING / MONITORING AGENCY NAME(S) AND ADDRESS(ES)

Headquarters, US Army Corps of Engineers
Washington, DC 20314-1000

10. SPONSOR/MONITOR'S ACRONYM(S)

USACE

11. SPONSOR/MONITOR'S REPORT NUMBER(S)

12. DISTRIBUTION / AVAILABILITY STATEMENT

Approved for public release; distribution is unlimited.

13. SUPPLEMENTARY NOTES

14. ABSTRACT

Operating vehicles in extremely cold environments is a significant problem for not only the public but also the military. The Department of Defense has encountered issues when trying to reliably cold start large, heavy-duty military vehicles, specifically the M1126 Stryker Combat Vehicle, in cold regions. As noted in previous work, the issue stems from the current battery technology's limited temperature range. This current project utilized the protocol established in the previous phase to evaluate next-generation lithium-ion battery technologies for use in cold regions. Selected battery technologies met necessary military specifications for use in large military combat vehicles and were evaluated using a mechanical load system developed in previous work to simulate the starting of a Stryker engine. This work also evaluated the performance of the existing battery technology of a Stryker under Alaskan winter temperatures, which will verify the accuracy of the simulated cold room testing on the mechanical load system. The results of the tests showed that while the system was able to reliably operate down to −20°C, the battery management system encountered challenges at the lower end of the temperature range. This technology has a potential to reliably support cold regions operations but needs further evaluation.

15. SUBJECT TERMS

Batteries; Cold regions; Energy; Lithium ion batteries--Effect of temperature on; Lithium-ion; Low temperature; Mobility; Resilience; Stryker; Vehicles, Military

16. SECURITY CLASSIFICATION OF:			17. LIMITATION OF ABSTRACT	18. NUMBER OF PAGES	19a. NAME OF RESPONSIBLE PERSON
a. REPORT	b. ABSTRACT	c. THIS PAGE			19b. TELEPHONE NUMBER (include area code)
Unclassified	Unclassified	Unclassified	SAR	52	